



Evaluation and Calibration of Clarity Node S Low-Cost Sensors in Lubbock, Texas

John Garber¹ and Karin Ardon-Dryer¹

¹Department of Geosciences, Texas Tech University, Lubbock TX, USA 79409.

5

Correspondence to: Karin Ardon-Dryer (karin.ardon-dryer@ttu.edu)

Abstract. Aerosol particles, also known as Particulate Matter (PM), have a profound impact on human health, air quality, the weather, and climate. PM can be measured using a variety of measuring techniques and instruments, notably reference-grade instruments and Low-Cost Sensors (LCS). Although Low-Cost Sensors allow for a higher resolution network, some have accuracy issues and reliability when compared to reference-grade units, which prompts the need to develop a calibration. This work, which is part of the Lubbock Environmental Action Plan (LEAP) for Communities, aims to provide information on air quality levels across the city of Lubbock using Clarity Node S sensors. In this study, which is the first step of the work, an evaluation and calibration of four Clarity Node S sensors was performed. The Clarity Node S sensors were selected for this project due to the sensors' ability to operate without a power or Wi-Fi source. Good agreement was found between the sensors when they were collocated with each other from March to May 2024 on the Aerosol Research Observation Station (AEROS). Next, one LEAP unit was collocated at AEROS with a reference unit, and different calibration tests were performed for the three PM concentrations measured by the Clarity units (PM₁, PM_{2.5}, and PM₁₀, particles with diameters <1, 2.5, and 10µm, respectively). The selected calibration was developed and implemented for all four LEAP units. The calibrated LEAP units were then collocated near two different reference units for a duration of eight months (July 2024 to February 2025), and a comparison was performed. While one reference unit showed a good agreement with three LEAP units, the other reference units were very different from the collected LEAP unit.

10

15

20

1 Introduction

Atmospheric Particulate Matter (PM) generated by natural and anthropogenic sources is defined by the particle aerodynamic diameter. Three size definitions that are most commonly used are PM₁, PM_{2.5}, and PM₁₀ (particles with diameters <1, 2.5, and 10µm, respectively). High concentrations of PM produce negative impacts on air quality (Huang et al., 2009; Goyal et al., 2010; Rovira et al., 2020) and to the Economy (Zhang et al., 2008; Yang et al., 2019; Nguyen et al., 2021). High PM concentrations also impact the global radiation balance (Shim et al., 2025), cloud formation (Bangert et al., 2012; Alizadeh-Choobari and Gharaylou, 2017), the Earth's climate (Megaritis et al., 2014; Fiore et al., 2015), and the atmospheric vertical electric field (Zhang et al. 2018; Ardon-Dryer et al. 2022a). High concentrations of these three PM sizes are known to have a

25



30 negative impact on human health due to their size and ability to penetrate into the human body (Kampa and Castanas, 2008; Valavanidis et al., 2008; Shaughnessy et al., 2015). Therefore, it is important to monitor the concentrations of PM of all sizes.

Two different official methods are commonly used to measure PM concentrations in Air Quality Monitoring Stations (AQMS): The Federal Reference Method (FRM) and the Federal Equivalent Method (FEM). FRM operates via gravimetric analysis, where ambient particulates are size-sorted through various air inlets before they accumulate on a filter for a 24-hour period (Eisner and Wiener, 2002; Rees et al., 2004; Clements and Vanderpool, 2019). The PM concentration is then measured by calculating the weight difference between the filter weights before and after particle collection (Rees et al., 2004). FRM provides reliability and consistency and is used as a reference for the calibration of other monitors (Eatough et al., 2001; Clements and Vanderpool, 2019). Two examples of networks that utilize the FRM are the Chemical Speciation Network (CSN), with sites located mainly in urban and suburban settings, and the Interagency Monitoring of Protected Visual Environments (IMPROVE), located in remote and rural sites (Malm et al., 1994; Solomon et al., 2014). However, these monitors are large, expensive to purchase and to operate, fixed to one location, and require trained personnel as well as manual labor for filter measurement and maintenance (Clements and Vanderpool, 2019). The FRM also has a low time resolution (one measurement per day), and measurements in CSN and IMPROVE are normally made every three days, meaning these networks may fail to detect PM events that occur in between measurements (Delgado-Saborit, 2012; Ardon-Dryer et al., 2023). The FEM method provides continuous measurements, including the Beta Attenuation Mass Monitors (BAMs), Tapered Element Oscillating Microbalance (TEOM), and an optical monitor. The BAM measures mass concentration using the principle of beta ray attenuation, where the beta rays travel through the filter tape and are detected with a scintillation detector. The ratio (of beta rays) between the filter tape after PM collection to those measured before particle collection determines the mass density of collected PM on the filter tape (Wedding and Weigand, 1993; Chueinta and Hopke, 2001; Met One, 2019). The TEOMs utilize a hollow glass element that oscillates at a specific frequency using feedback electronics or magnets. An increase in particle mass concentration decreases the frequency of the oscillating element, allowing the unit to calculate mass concentrations accordingly (Patashnick and Rupprecht, 1991; Mignacca and Stubbs, 1999). The optical monitor method measures the particles using light scattering technology with either a nephelometer or photometer (Hagan and Kroll, 2020). These sensors allow for the measurement of particle mass concentration and size distribution (Grimm and Eatough, 2009; Hagan and Kroll, 2020). An example of such a unit is the GRIMM/DURAG EDM-180. Due to their large size and high cost (Clement and Vanderpool, 2019; Hagan and Kroll, 2020), these different FEM monitors are limited in their spatial and geographical coverage. Even with the available networks (AQMS, CSN, and IMPROVE) for PM measurements, there are still many areas with low spatial resolution (Ardon-Dryer et al., 2023; Roque et al., 2025). PM values measured in one neighborhood may not reflect the PM values in a nearby neighborhood (Ardon-Dryer et al., 2020; Hagan and Kroll, 2020; Ardon-Dryer and Aziz, 2025). The need to improve the spatiotemporal resolution of PM measurements and provide the public with accessible information regarding the local air quality led to the development of low-cost sensors (LCS).



LCS are smaller, cheaper, and more portable compared to the FRM/FEM counterparts, which allow for use in high spatial and
65 temporal PM monitoring networks (Ardon-Dryer et al., 2020; Raheja et al., 2023; Zico da Costa et al., 2024). Many of the
low-cost sensors contain either a Plantower PMS5003 or PMS6003 sensor, which are light-scattering instruments that are
classified as particle counters (Ouimette et al., 2022). Some of the low-cost sensors also contain internal instruments to measure
internal temperature (T), relative humidity (RH), and pressure (P) (Clarity, 2023; PurpleAir, 2023). While the utilization of
LCS has become increasingly common, with thousands deployed across the world, there are still many uncertainties regarding
70 the reliability and quality of the collected data (Spinelle et al., 2015; Lewis and Edwards, 2016). To reduce costs, companies
construct these sensors using cheaper parts, which may impact the quality control, assurance, and signal transparency of the
product, making them potentially inadequate for accurate PM measurement (Barkjohn et al., 2021; Papapostolou et al., 2017).
LCSs can produce overestimations of PM concentrations due to the hygroscopic growth of the particle, typically during high
RH conditions (Crilley et al., 2018). Some LCSs can also underestimate the PM concentration in low RH conditions
75 (Chakrabarti et al., 2004; Soneja et al., 2014). While most LCSs show high correlations between sensors (of the same type),
the uncalibrated or uncorrected LCS measurements normally have low correlation and high error when compared to a reference
FEM or FRM monitor (Ardon-Dryer et al., 2020; Zaidan et al., 2020; Raheja et al., 2023). Different regression methods have
been used to correct and evaluate the performance of these low-cost sensors when collocated and compared with a reference
monitor. Some of the regression methods used to improve LCS measurements are Linear (LR), Multivariate (MLR), Random
80 Forest (RF), Ordinary Least Squares (OLS), and Quantile (Ardon-Dryer et al., 2020; Barkjohn et al., 2021; Raheja et al., 2023).
Some of the corrections consider other variables that can impact LCS PM measurements, including T and RH (Jiao et al.,
2016; Ardon-Dryer et al., 2020; Nobell et al., 2023) or even dew point Temperature (Barkjohn et al., 2021).

This research project is part of the Lubbock Environmental Action Plan (LEAP) for Communities, a project funded by the US
85 Environmental Protection Agency (EPA grant # 02F28601). The LEAP project aims to investigate the air quality levels across
the city of Lubbock, Texas. As there is only one single reference sensor, operated by the Texas Commission of Environmental
Quality (TCEQ), in this area that only measures $PM_{2.5}$. This sensor is located on the eastern edge of Lubbock near an
agricultural field, away from urban or residential areas. As part of LEAP, multiple Clarity Node S units and one reference
monitor were purchased for this project. This study will present the first step of this project, which includes the calibration
90 process, as well as an eight-month analysis and comparison of collocated Clarity Node S units with two reference units at two
locations.

2 Methodology

2.1 Research area

This research took place in Lubbock, Texas, an urban area (population ~300,000) surrounded by rural agriculture (primarily
95 cotton). Located in the Panhandle on the Southern High Plains Plateau of West Texas, approximately 1 km above sea level.



The climate is characterized by a semi-arid climate, with annual precipitation (from 2000 to 2024) of 472 ± 172 mm, mainly during the late spring to summer months (NWS, 2025). The flat terrain, low vegetation cover, and sparse which offer no obstruction from the wind, lead to the formation of dust events. The area experiences many dust events (Kelley and Ardon-Dryer, 2021; Robinson and Ardon-Dryer, 2024) that lead to high PM concentrations (Kelley and Ardon-Dryer, 2021; Ardon-Dryer and Kelley, 2022; Robinson et al., 2024).

2.2 Instrumentation used in this study

This study includes four LCS units, Clarity Node S sensors, and two reference units: a GRIMM/DURAG EDM-180 and a Met One BAM-1022 unit, operated by TCEQ.

105 The Clarity Node S sensor (Clarity from here on) uses a Plantower PMS6003 dual laser light scattering instrument to monitor and measure PM_{10} , $PM_{2.5}$, and PM_1 (Nobell et al., 2023). PM concentrations range from 0 to $1000 \mu g m^{-3}$ at a resolution of $1 \mu g m^{-3}$ (Clarity, 2023). The sensor also contains a Bosche BME280 sensor that measures P, T, and RH (Clarity, 2023). The Clarity sensor has an operational temperature that ranges from $-10^{\circ}C$ to $55^{\circ}C$ and an operational RH range of 10% to 98%. While the sensor can measure particles at high RH conditions, it does not have a built-in dryer to reduce particle hygroscopic growth (Clarity, 2023). The Clarity Node S sensor was selected for this project due to its ability to operate without the need for external power and Wi-Fi, by using a built-in solar panel and an SD card port. This allows the sensor to communicate data over cellular networks while deriving all its operational power from incoming solar radiation, allowing it to conduct analysis and comparison at multiple locations. Each Clarity sensor received the name LEAP with a number (e.g., LEAP01, LEAP02).

115 The GRIMM/DURAG EDM-180 instrument is an optical sensor (featuring an internal 600 nm laser) that measures mass concentration of PM_{10} , $PM_{2.5}$, and PM_1 , in a range of $0-1000 \mu g m^{-3}$ as well as particle concentrations using 31 bin sizes from $0.25 \mu m$ to $32 \mu m$. The unit operates at a flow rate of $1.2 L min^{-1}$ and can count up to 3 million particles per Liter. The EDM-180 is connected to a 1.5-meter sample pipe featuring a TSP head, an integrated Nafion dryer, and a water drain, which minimizes hygroscopic effects. The EDM-180 is placed in an air-conditioned, weatherproof housing (Model 199) that allows full operation in a variety of weather conditions, including an operating ambient temperature of $-20^{\circ}C$ to $60^{\circ}C$ and an ambient relative humidity of 0% to 95% (GRIMM/DURAG, 2020). The unit is approved for PM_{10} according to the European Union Council Directive (EUCD-EN12341, 1998) and approved for $PM_{2.5}$ according to the US-EPA and equivalent to EUCD (EN14907, 2005). The EDM-180 continuously collects and stores PM data at 1-minute intervals, which are then converted to hourly and daily values using MATLAB code.

125

The Met One BAM-1022, operated by TCEQ and the only reference monitor in Lubbock with publicly available data, was also used in this project. Measurements from the BAM-1022 unit were downloaded from the TCEQ website (TCEQ, 2025). The BAM-1022 sensor measures the mass concentration of $PM_{2.5}$ using beta rays emitted from radioactive decay of carbon-



14 (¹⁴C; Met One, 2025). Particles are collected on filter tape, which sits between the beta emitter and detector, and is rolled
130 at a designated period of 1 hour. The BAM-1022 operates at a flow rate of 16.7 L min⁻¹ and it uses an internal heater to reduce
hygroscopic growth of collected particles. The unit has a measurement range of -15 µg m⁻³ to 10000 µg m⁻³ and has a data
resolution of 1 µg m⁻³. The BAM-1022 unit has an operational temperature range of -30°C to 50°C, along with a non-
condensing operational relative humidity range of 0% to 90%. The unit meets the Class III certification from the US EPA
(EQPM-1013-209) for FEM outdoor measured PM_{2.5}. This specific site has EPA site number 48-303-1028 and has been
135 operating since August 13, 2016. In July 2018, the TEOM unit (A Tapered Element Oscillating Microbalance R & P Model
1400a) was replaced with the current BAM unit (Stephanie Ma, TCEQ personal communication). The BAM-1022 collects and
submits data continuously at intervals of one hour and can be accessed through the TCEQ website (TCEQ, 2025).

Meteorological information (such as T and RH) was taken from Clarity's internal sensors. T and RH measurements from the
140 West Texas Mesonet (WTM) station LBBW2, located 2.9 km from the Aerosol Research Observation Station (AEROS), were
provided by the WTM team (West Texas Mesonet, 2025). The WTM is a network of >155 meteorological stations across the
West Texas region that measure above-ground standard meteorological parameters such as temperature, wind, pressure,
radiation, and humidity, as well as below-ground measurements of soil moisture and temperature at multiple depths (West
Texas Mesonet, 2025). Additional meteorological measurements were taken from the Automated Surface Observation Stations
145 (ASOS), which are operated by the National Weather Service (NWS), and located at Lubbock International Airport, 9.8 km
from AEROS. The meteorological measurements available to the public as meteorological aerodrome reports (METARs)
include 5-minute to 1 h measurements of T, dew point (dT), RH, wind speed, wind direction, wind gust, pressure, visibility,
and precipitation, as well as “present weather code”. The ASOS data was retrieved from the Iowa State Mesonet (2025).

150 At the first step, a collocation period of all four Clarity sensors took place at AEROS, a research station located on the rooftop
of the Electrical Engineering building at Texas Tech University (see more information on AEROS: Ardon-Dryer et al., 2022;
Ardon-Dryer and Kelley, 2022). The Clarity Node S sensors were placed on the AEROS filter sampler unit on March 4, 2024,
at 13:00 CDT Central Daylight Time, defined as local time (LT), from here on. By 14:00 LT, all sensors were deployed at
AEROS. Sensors were active at AEROS until May 21, 2024, at 23:00 LT, when the units were removed and prepared for
155 deployment around the city. During these 78 days, the sensors measured at a default rate of once every 15 minutes. Hourly
averages of PM concentrations were calculated from these raw measurements, and then sensors were compared with each
other to determine overall sensor network behavior and identify outliers among the Clarity units. On May 23, 2024, all sensors'
measurement rates were changed to the fastest data-collection intervals, which are 3 to 4-minute intervals.

160 In the second step (from May 24 to June 30, 2024), one Clarity unit (named LEAP01) was left in AEROS near the reference
unit EDM-180, and corrections and calibration for the Clarity units were developed. One Clarity unit (LEAP02) was placed
near the TCEQ (BAM-1022) unit (on May 24, 2024), while the remaining Clarity units (LEAP41 and LEAP42) were placed



back on AEROS (only on July 2, 2024), near LEAP01 (as shown in Fig. 1). Comparison between each LEAP unit to the collocated reference unit was then performed to evaluate the calibration and correction developed.



165

Figure 1: Map showing the location of the study area. Observation of the Aerosol Research Observation Station (A), which held the EDM-180, and the filter sampler unit that holds the three metal racks for the three Clarity Node sensors (and LEAP01, LEAP41, and LEAP42), as well as the TCEQ site (B), with the BAM-1022 and one Clarity Node sensor (LEAP02).

2.3 Software and Statistical Analysis used

170 Different calculations were made using Excel and MATLAB codes. These calculations include hourly average \pm standard deviation (SD) values. To evaluate the similarities and differences between each sensor, different calculations and comparisons were performed using MATLAB and Excel. These include R-squared (R^2), root-mean-square error (RMSE), mean absolute error (MAE) values, as well as the best-fit information, including the slope and Intercept.

3 Results

175 3.1 Intercomparison of the four clarity sensors at AEROS

Comparisons of the four Clarity units with each other were based on linear regression, where R^2 , RMSE, MAE, and the slope values between the sensors were used. Overall, the Clarity units demonstrated good agreement with each other for each of the examined PM sizes (raw concentrations for PM_1 , $PM_{2.5}$, and PM_{10}) when 1881 hours were used, as shown in Fig. 2. Comparison between these four Clarity units for PM_1 values resulted in R^2 values that ranged from 0.99 to 1.0, with an average of 0.99 ± 0.003 . RMSE values ranged from 0.43 to $0.64 \mu g m^{-3}$. The average RMSE value was $0.57 \pm 0.1 \mu g m^{-3}$, the MAE average was $0.37 \pm 0.08 \mu g m^{-3}$, and it ranged from 0.27 to $0.44 \mu g m^{-3}$. The slope ranged from 0.93 to 1.19, while the average slope was 1.06 ± 0.11 . $PM_{2.5}$ concentration among these four units had an average R^2 value of 0.99 ± 0.002 , RMSE values ranged from 0.69 to $1.0 \mu g m^{-3}$, the average RMSE value was $0.87 \pm 0.12 \mu g m^{-3}$, the MAE average was $0.54 \pm 0.09 \mu g m^{-3}$, and it ranged from 0.43 to $0.64 \mu g m^{-3}$. The slope ranged from 0.9 to 1.19, with an average of 1.04 ± 0.11 . Comparison of PM_{10} concentration
185 resulted in an R^2 value of 0.98 to 0.99, with an average of 0.98 ± 0.004 . RMSE values ranged from 1.11 to $1.75 \mu g m^{-3}$, with an average RMSE value of $1.4 \pm 0.26 \mu g m^{-3}$; the MAE average was $0.86 \pm 0.14 \mu g m^{-3}$, and it ranged from 0.71 to $1.03 \mu g m^{-3}$.



3. The Slope ranged from 0.8 to 1.2, with an average of 0.98 ± 0.15 . Comparisons were also performed between the units for T and RH measurements, where >1500 hours were used for each comparison. R^2 values for the T measurements between all units ranged from 0.992 to 1.0; the average R^2 value was 1.0 ± 0.003 . RMSE ranged from 0.15 to 0.66°C , with an average RMSE value of $0.46 \pm 0.22^\circ\text{C}$; MAE ranged from 0.1 to 0.46°C , with an average of $0.32 \pm 0.17^\circ\text{C}$. The average slope was 1.0 ± 0.01 ; it ranged from 1.0 to 1.02. Similar findings were found for the comparison of RH, where the average R^2 value was 1.0 ± 0.000 . RMSE ranged from 0.51 to 1.2%, with an average of $0.92 \pm 0.031\%$. The average MAE was $0.65 \pm 0.23\%$; it ranged from 0.35 to 0.84%. The average slope was 0.99 ± 0.01 , and it ranged from 0.98 to 1.0. These results highlighted the fact that the Clarity units were similar to each other. Additional studies found high comparability between Clarity units, with good agreement and high correlation values (Ramiro et al., 2019; Zaidan et al., 2020; Byrne et al., 2024). Based on this agreement, LEAP01 remained on AEROS, LEAP02 was moved to the TCEQ site, and LEAP41 and LEAP42 returned to AEROS in early July.

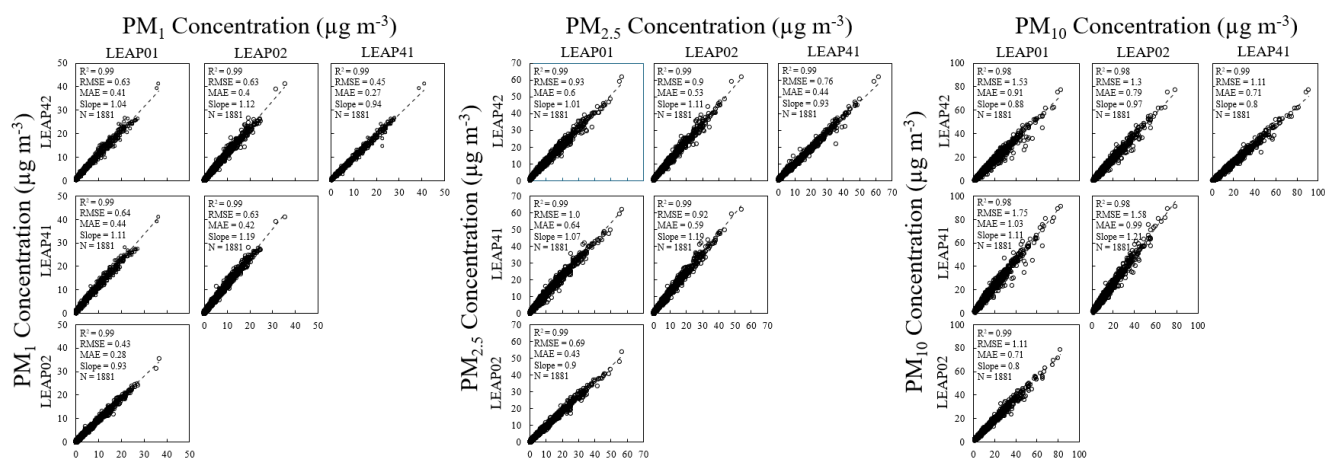


Figure 2: Comparison of RAW PM values between the four clarity units at AEROS, for PM₁ (A), PM_{2.5} (B), and PM₁₀ (C).

200

3.2 Development of Correction and Calibration of LEAP

3.2.1. Calibration correction for PM_{2.5} values

Comparison between the PM_{2.5} measured by uncorrected (raw) LEAP01 and the EDM-180 values (Fig. 3A) highlighted the need to correct the LEAP sensors. Hourly PM_{2.5} values measured by LEAP01 overestimated many of the EDM-180 values. Comparison between the raw LEAP01 PM_{2.5} values to those measured by the EDM-180 resulted in an R^2 value of 0.66, an RMSE of $5.3 \mu\text{g m}^{-3}$, an MAE of $3.4 \mu\text{g m}^{-3}$, and a slope of 1.33. The AQ Sensor Performance Evaluation Center (AQ-SPEC) evaluated the performance of raw PM_{2.5} values from the Clarity sensor using a reference unit under laboratory and field conditions in the Los Angeles area. AQ-SPEC evaluation showed a very good comparison under laboratory conditions, with an R^2 value of 0.99, but with a slightly lower R^2 value (0.73-0.76) under field conditions (AQ-SPEC 2018a,b). According to



210 AQ-SPEC (2018b), the slope for the field comparison did not show an overestimation of the Clarity $PM_{2.5}$ values. However,
our analysis found an overestimation of the Clarity raw hourly $PM_{2.5}$ values, with a slope of 1.33, similar to those found in
previous studies (Escobar-Diaz et al., 2021; Nobell et al., 2023; Raheja et al., 2023). For example, Escobar-Diaz et al. (2021)
found a slope of 1.4, and Raheja et al. (2023) found that the raw Clarity $PM_{2.5}$ values had significantly higher peaks than those
measured by the reference unit. These findings highlight the need to perform a calibration correction to the raw Clarity values.

215

Different calibration corrections were developed to correct the Clarity $PM_{2.5}$ values. The calibration was performed between
LEAP01 and EDM-180, since both were collocated at AEROS between May 24 to June 30, 2024, and there were 912 hours
of concurrent measurements between the two. All corrections were based on LR or MLR. A summary of all examined
regressions and corrections, including R^2 , RMSE, MAE, and slope, is presented in Fig. 3.

220

The first correction was based on the LR between the EDM-180 to LEAP01 $PM_{2.5}$ values. This regression resulted in an R^2
value of 0.66, an RMSE of $3.98 \mu\text{g m}^{-3}$, and an MAE of $2.57 \mu\text{g m}^{-3}$, slightly better than the comparison of the raw values.
Next, MLR was performed between $PM_{2.5}$ measurements of EDM-180 to LEAP01, with meteorological measurements such
as T and/or RH. Three different locations with hourly T and RH measurements were tested: the first WTM LBBW2 station,
225 located 2.9 km from AEROS, the second meteorological station ASOS, 9.8 km from AEROS, and the third, an internal T and
RH measurements from the LEAP01 sensor. Comparison between the three sites showed that T and RH measurements were
very similar to each other, with $R^2 > 0.89$ for T and $R^2 > 0.91$ for RH (data not shown). The first MLR tests included the EDM-
180 and LEAP01 $PM_{2.5}$ values as well as T measurements (Fig. 3C-E). All regressions were similar, even when T
measurements were taken from different locations. R^2 values for these MLRs were 0.66, RMSE was 3.97 to $3.98 \mu\text{g m}^{-3}$, and
230 the MAE ranged from 2.57 to $2.59 \mu\text{g m}^{-3}$ (Fig. 3C-E). A similar test was performed with RH measurements instead of T (Fig.
3F-H). There was a slight improvement in the correction when RH was used instead of T. R^2 increased to 0.68, and lower
RMSE and MAE were found (3.77 to $3.78 \mu\text{g m}^{-3}$ for RMSE and 2.5 to $2.58 \mu\text{g m}^{-3}$ for MAE; Fig. 3F-H).

Since many of the studies that use Clarity sensors indicated that the best $PM_{2.5}$ calibration was achieved when the correction
235 used both T and RH measurements (Zaidan et al., 2020; Nobell et al., 2023; Raheja et al., 2023; Attey-Yeboah et al., 2025),
an MLR correction using the $PM_{2.5}$ measurements from the EDM-180, as well as measurements of both T and RH, was
performed. Measurements from each of the three locations, WTM, ASOS, or LEAP01, were used. The usage of this MLR
slightly improved the correlation values. The measurements of T and RH from the WTM station resulted in an R^2 value of
0.68, RMSE of $3.77 \mu\text{g m}^{-3}$, and an MAE of $2.49 \mu\text{g m}^{-3}$ (Fig. 3I). Slightly higher R^2 , and lower RMSE and MAE values were
240 found when the T and RH were used by the ASOS or by the LEAP01 internal sensor. R^2 values for both MLR were 0.7, RMSE
was $3.6 \mu\text{g m}^{-3}$, and MAE was $2.41 \mu\text{g m}^{-3}$ (Fig. 3J-K). All cases resulted in a good slope (~ 1.0). Many studies use the internal
T and RH measurements for the correction of the sensors (Raheja et al., 2023; Nobell et al., 2023; Attey-Yeboah et al., 2025).
However, other studies indicated that there is a need to correct the T and RH measurements before these could be used for the



correction of the PM values (Zaidan et al., 2020). Nobell et al. (2023) used MLR with T and RH, which improved their R^2
245 from 0.87 to 0.97, higher than the R^2 found in this study. Yet the RMSE values found in Nobell et al. (2023) were much higher
than those measured in this study. Raheja et al. (2023), on the other hand, who also used the internal T and RH measurements
in their MLR, found similar improvement in their correlation as the one found in this study; where the R^2 improved from 0.69
to 0.73, and MAE decreased from 13.68 to 2.58 $\mu\text{g m}^{-3}$. We were hoping for a better improvement in the calibration, and we
250 were wondering if the fact that this study was performed in a semiarid area, which experiences dust events, could impact the
calibration.

Lubbock is prone to dust events, especially in late winter and spring months (Kelley et al., 2020; Robinson and Ardon-Dryer,
2024; Robinson et al., 2024). Observations of PM_{10} - $\text{PM}_{2.5}$ measured by EDM-180 allowed the detection of times when dust
particles were present in the air, even during this development calibration period (Fig. S1A). Observations of $\text{PM}_{2.5}$ from EDM-
255 180 and LEAP01 (raw values) highlight that some dust events were detected by EDM-180 ($\text{PM}_{2.5}$ increased) but were not
detected by the raw LEAP01 $\text{PM}_{2.5}$ values (Fig. S1B). We were wondering if using PM_{10} values measured by EDM-180 will
improve the correction of $\text{PM}_{2.5}$ for Clarity units. To the best of our knowledge, no previous study includes PM_{10} values to
make corrections for $\text{PM}_{2.5}$, perhaps since there is a limited number of locations with reference units that contain both PM
sizes (Ardon-Dryer et al., 2023). Previous studies (e.g., Analitis et al., 2020) used PM_{10} to develop a model to predict $\text{PM}_{2.5}$
260 concentrations where those were not directly measured. Therefore, for the next MLR, $\text{PM}_{2.5}$ and PM_{10} values from the EDM-
180 were used in addition to LEAP internal T and RH measurements (since no significant difference was found when the other
sites, WTM or ASOS, were used). This MLR produced the highest R^2 value and the lowest RMSE and MAE values (shown
in Fig. 3L). R^2 value was 0.94, RMSE was 1.41 $\mu\text{g m}^{-3}$, and MAE was 0.96 $\mu\text{g m}^{-3}$. We noticed that there were 15 hours (15:00
LT on May 25 until 8:00 LT on May 26) that contained high PM values when LEAP01 values did not detect any increase in
265 PM values. We decided to remove these 15 hours from the data and run the same MLR again, now with 897 hours instead of
912. Removal of these 15 hours improved the regression values. R^2 increased to 0.95, RMSE reduced to 1.26 $\mu\text{g m}^{-3}$, and MAE
dropped to 0.86 $\mu\text{g m}^{-3}$ (Fig. 3M). The MLR of this calibration was corrected using the following equation:

$$LEAP_{TTUcorrect,PM2.5} = \frac{LEAP_{PM2.5} - INT - (LEAP_T \times T^*) - (LEAP_{RH} \times RH^*) - (EDM_{PM10} \times EDM_{PM10}^*)}{LEAP_{PM2.5}^*} \quad (1)$$

Where $LEAP_{PM2.5}$ represents the uncorrected (raw) LEAP $\text{PM}_{2.5}$ hourly values, $LEAP_T$ and $LEAP_{RH}$ are LEAP hourly T ($^{\circ}\text{C}$)
270 and RH (%) values. EDM_{PM10} is the PM_{10} hourly value measured by the EDM-180. INT represents the intercept coefficient
value, which is -5.77. While T^* , RH^* , $LEAP_{PM2.5}^*$, and $LEAP_{PM10}^*$ are coefficients developed in this MLR, which are 0.099,
-0.00042, 2.12, and -2.89, respectively. This calibration correction was selected as the final correction and will be named TTU-
calibration from here on.

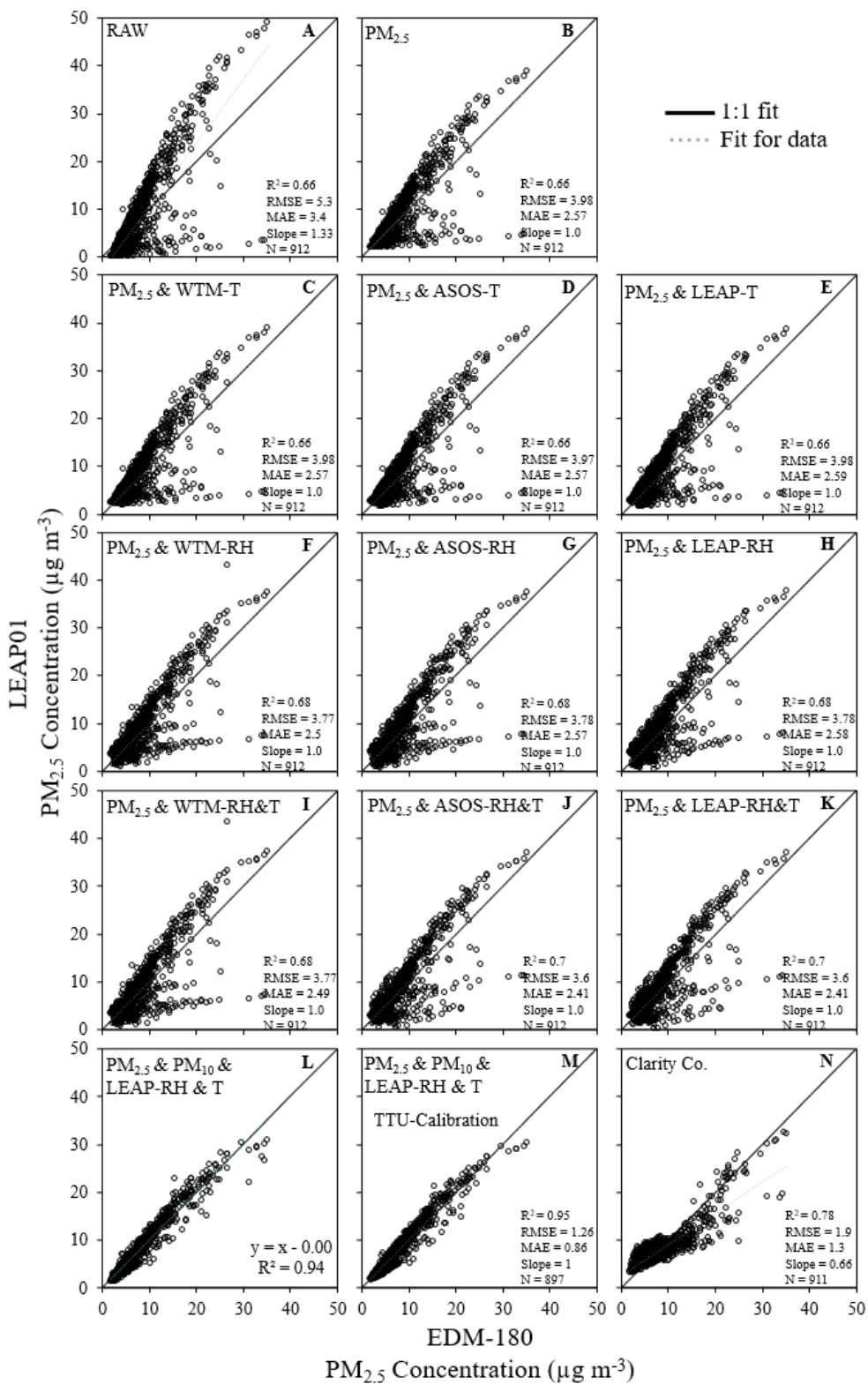
275 The Clarity Movement Co. (Clarity Co.) also developed a correction for the uncorrected raw LEAP $\text{PM}_{2.5}$ measurements and
provided us with the information and corrected values. For this correction, Clarity Co. used measurements from July 2 to



280 August 31, 2024, since it required having multiple LEAP units active with the reference unit. Three LEAP units were active on AEROS at that time (LEAP01, LEAP41, and LEAP42) and were used with EDM-180 to develop the Clarity Co. Calibration (CC). Clarity averaged all LEAP measurements for every measured parameter and pulled from a random selection of 80% of the days used in the calibration period for each model they developed. After finding the best-performing model, Clarity Co. evaluated the model by applying it to the remaining 20% of days from this period that weren't selected to develop this calibration. Clarity Co. tested the performance of the hourly and daily average comparison of the model with the EDM-180 to the performance of the hourly and daily average comparison between the raw LEAP measurement and the EDM-180 during this 20% period. CC was based on MLR that included $PM_{2.5}$ and PM_{10} values from the LEAP units, in addition to LEAP
285 internal RH measurements. The CC calibration utilized this equation:

$$LEAP_{CC_{correct,PM_{2.5}}} = \frac{LEAP_{PM_{2.5}} - INT - (LEAP_{RH} \times RH^*) - (LEAP_{PM_{10}} \times LEAP_{PM_{10}}^*)}{LEAP_{PM_{2.5}}^*} \quad (2)$$

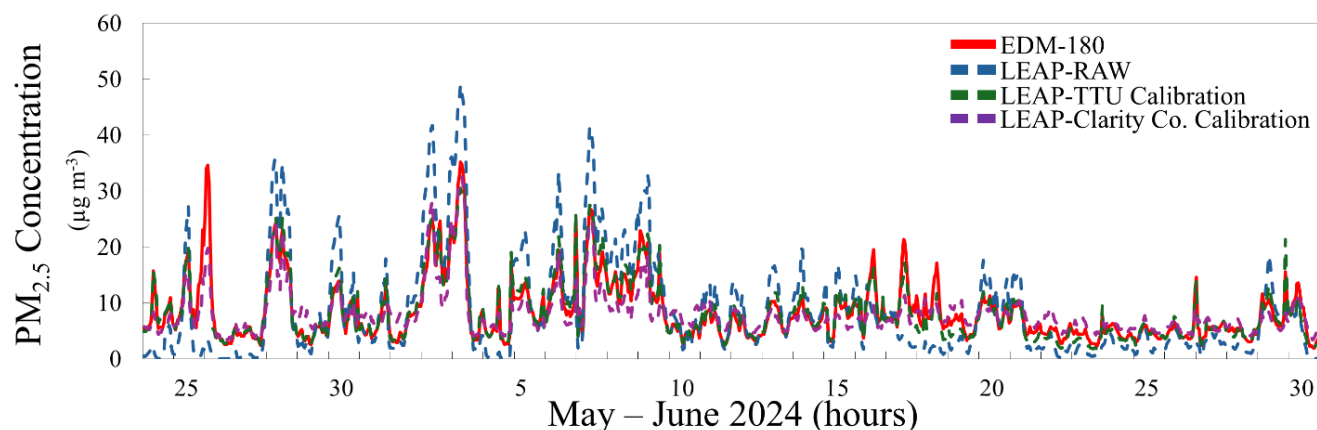
Where $LEAP_{PM_{2.5}}$, $LEAP_{PM_{10}}$, and $LEAP_{RH}$ represent the average LEAP $PM_{2.5}$, PM_{10} , and RH hourly values. INT represents the interception, which is -0.18. The coefficient value of $LEAP_{RH}^*$ is 0.047, $LEAP_{PM_{10}}^*$ is 1.70, and $LEAP_{PM_{2.5}}^*$ is -1.67. According to the Clarity Co. calibration report (data not shown), this regression improved the raw LEAP01 values R^2 value
290 from 0.39 to 0.8, the RMSE from $7.07 \mu g m^{-3}$ to $1.93 \mu g m^{-3}$, and the MAE from $5.23 \mu g m^{-3}$ to $1.58 \mu g m^{-3}$. The LEAP01 hourly $PM_{2.5}$ values based on the Clarity Co. calibration correction was then compared to the EDM-180 $PM_{2.5}$ values for the period of May 24 to June 30, 2024, time used during the TTU correction development period, as shown in Fig. 3N. While the CC provided some statistical improvement (R^2 was higher, 0.78, with lower RMSE and MAE values, 1.9 and $1.3 \mu g m^{-3}$, respectively) for LEAP01 $PM_{2.5}$ raw values, it did not outperform the TTU calibration (Eq. 1).





300 **Figure 3: Scatter plots between EDM-180 to the raw LEAP01 PM_{2.5} values (A), calibration of LEAP01 PM_{2.5} values based on EDM-180 PM_{2.5} values (B), calibration based on EDM-180 PM_{2.5} values and WTM T measurements (C), EDM-180 PM_{2.5} values and ASOS T measurements (D), EDM-180 PM_{2.5} values and LEAP T measurements (E), calibration based on EDM-180 PM_{2.5} values and WTM RH measurements (F), EDM-180 PM_{2.5} values and ASOS RH measurements (G), EDM-180 PM_{2.5} values and LEAP RH measurements (H), calibration based on EDM-180 PM_{2.5} values and WTM T and RH measurements (I), EDM-180 PM_{2.5} values and ASOS T and RH measurements (J), EDM-180 PM_{2.5} values and LEAP T and RH measurements (K), calibration based on EDM-180 PM_{2.5} and PM₁₀ values with LEAP T and RH measurements (L), calibration based on EDM-180 PM_{2.5} and PM₁₀ values with LEAP T and RH measurements after removal of 15 hours of high PM, also known as TTU calibration (M) and calibration based on Clarity Co. calibration (N). The dashed line represents the best fit between the sensors, while the gray sash line represents the 1:1 line.**

305 To compare between the different calibrations, specifically TTU-calibration (Eq. 1) and the CC calibration (Eq. 2), we decided to observe the fluctuation of the hourly PM_{2.5} hourly values, for May 24 to June 30, 2024, based on the raw LEAP01 PM_{2.5} values, and those resulted by the TTU-calibration and the CC calibration as well as those measured by the EDM-180 (Fig. 4). Observations of the uncorrected LEAP values highlight the overestimation of the raw values. Comparison between the LEAP01 hourly PM_{2.5} values using the TTU-correction to those measured by the EDM-180 highlights how the TTU correction
310 improves the raw LEAP PM_{2.5} values. CC calibration did improve the performance of the raw values, yet it did not have a strong improvement as the one found when TTU-calibration was used. Although other studies used a correction developed by Clarity Co. for their study (Zico da Costa et al., 2024). They did not provide any information on these calibrations or comparisons with a collocated reference unit.



315 **Figure 4: Comparison of hourly averaged PM_{2.5} values for EDM-180 (red) and LEAP01 raw (blue), TTU calibration (green), and Clarity Co. calibration (purple) for May to June 2024.**

3.2.2. Calibration correction for PM₁ values

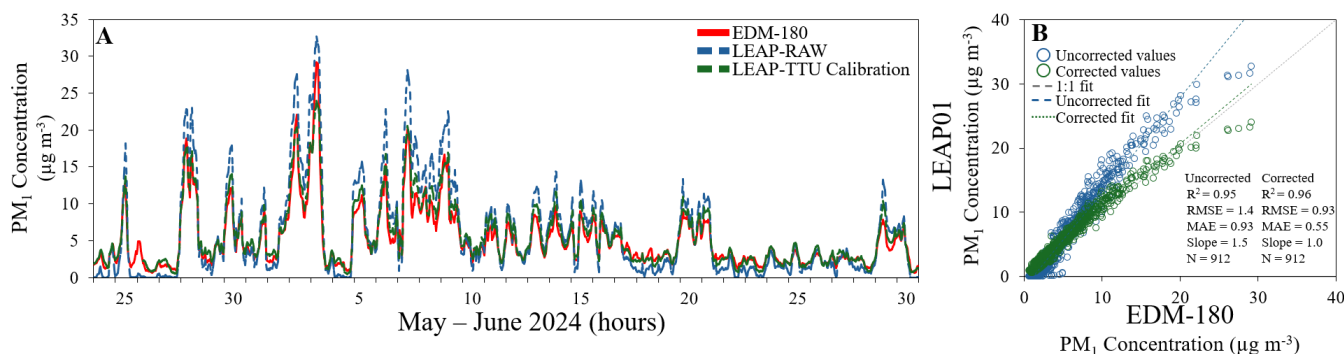
320 While most of the studies utilized Clarity sensors focused on PM_{2.5} concentrations, several present measurements of PM₁ concentrations (Ramiro et al., 2019; Liu et al., 2022). To the best of our knowledge, none of the studies that presented measurements of PM₁ using the Clarity sensors provide a calibration for PM₁ concentrations. While there is no official FRM or FEM, nor are there regulations available for PM₁ from any agency (EPA, 2024; Sufleta, 2025), we wanted to examine the Clarity PM₁ values and behavior. A comparison between the PM₁ concentrations measured by the raw LEAP01 and the EDM-



180 was performed (Fig. 5). The raw PM_1 values measured by LEAP01 seem to overestimate the EDM-180 PM_1 values (Fig. 325 5A). The overestimation of the raw PM_1 values compared to the EDM-180 was observed across most of the time measured. Similar overestimations of PM_1 values have been reported by studies that used Clarity sensors (Ramiro et al., 2019) as well as by those who used the Plantower PMS5003, the instrument used in the Clarity sensors (Molina Rueda et al., 2023). The comparison between the raw LEAP01 PM_1 to those measured by the EDM-180 resulted in R^2 value of 0.95, an RMSE of 1.36 $\mu g m^{-3}$, an MAE of 0.93 $\mu g m^{-3}$, but with a very high slope of 1.48 (Fig. 5B). Additional studies reported high agreement (high 330 R^2 value >0.9) between the PM_1 concentrations measured by Clarity (or PMS5003) to those of regulatory unit (Ramiro et al., 2019; Molina Rueda et al., 2023). Although a good agreement was found for PM_1 concentrations, the high slope highlighted the need to develop a correction for the PM_1 values. The first correction made was a linear regression only based on EDM-180 PM_1 values and LEAP01 PM_1 values. This correction, which was based on 912 simultaneous hours, resulted in an R^2 value of 0.95, an RMSE of 0.92 $\mu g m^{-3}$, an MAE of 0.63 $\mu g m^{-3}$, and a slope of 1. A slight improvement compared to the raw comparison. 335 Since the $PM_{2.5}$ regression demonstrated improvement with the usage of T and RH, a similar regression was developed for PM_1 . This MLR incorporated hourly EDM-180 and LEAP01 PM_1 values, as well as LEAP01 T and RH measurements. This MLR slightly improved the regression as it produced an R^2 value of 0.96, an RMSE of 0.84 $\mu g m^{-3}$, and an MAE of 0.58 $\mu g m^{-3}$. Utilizing the PM_{10} from the EDM-180 as an additional variable improved the regression and even lowered the RMSE and MAE (0.81 and 0.55 $\mu g m^{-3}$, respectively) values, although the R^2 value remained the same (R^2 of 0.96). Removal of the 15 340 hours from the high PM event, similar to the one used in Eq. 1, did not improve the MLR produced, as almost the exact R^2 , RMSE, and MAE were found (data not shown). Although no significant differences were found between the different MLR tested, we decided to keep consistent and use similar functions to those developed for $PM_{2.5}$. The final MLR developed to correct PM_1 values from LEAP included the EDM-180 hourly PM_1 and PM_{10} values as well as the LEAP T and RH hourly measurements (using the 897 hours, the same used for $PM_{2.5}$). This correction is utilized in this equation:

$$345 \quad LEAP_{TTUcorrectPM1} = \frac{LEAP_{PM1} - INT - (LEAP_T \times T^*) - (LEAP_{RH} \times RH^*) - (EDM_{PM10} \times EDM_{PM10}^*)}{EDM_{PM1}^*} \quad (3)$$

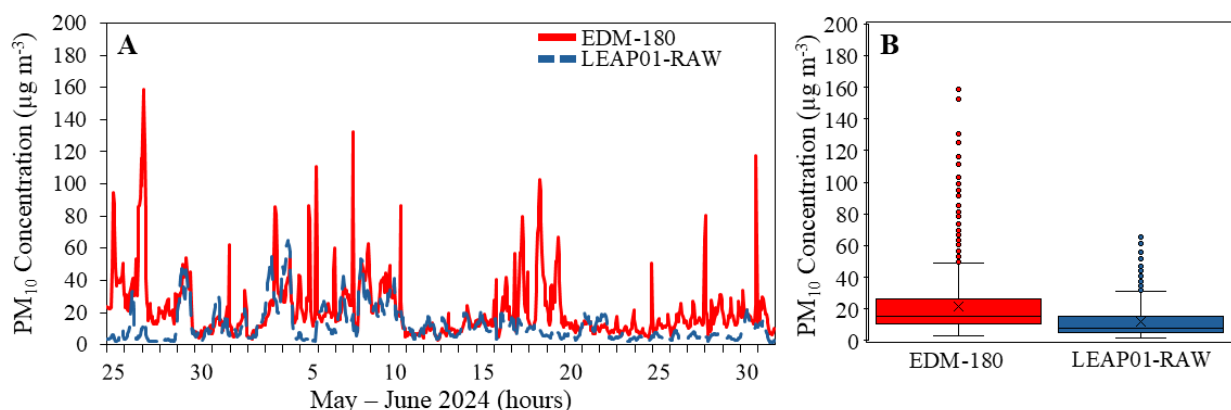
Where $LEAP_{PM1}$ represents the uncorrected LEAP PM_1 hourly values, $LEAP_T$ and $LEAP_{RH}$ are hourly T and RH values. EDM_{PM10} is the PM_{10} hourly value measured by the EDM-180. INT represents the intercept coefficient value, which is -5.77. While T^* , RH^* , $LEAP_{PM1}^*$, and $LEAP_{PM10}^*$ are coefficients developed in this MLR, which are 0.12, -0.015, 1.51, and -0.016, respectively. Observations of the corrected LEAP01 hourly PM_1 values seem similar to those measured by the EDM-180 (Fig. 350 5). Even the comparison between the LEAP01 hourly PM_1 values to those measured by the EDM-180 (Fig. 5B) highlights how the correction improves PM_1 values compared to the raw values, with the main impact seen for the slope values.



355 **Figure 5: Comparison of hourly averaged PM₁ values between EDM-180 to LEAP01 during May - June 2024. (A) Time series with EDM-180 (red), LEAP01 raw (blue), and TTU PM₁ calibration (green), as well as (B) scatter plots between EDM-180 to the raw and calibrated LEAP01 PM₁ values, with information on each regression comparison. The dashed line represents the best fit between the sensors, and the gray sash line represents the 1:1 line.**

3.2.3. Calibration correction for PM₁₀ values

360 Comparisons were also made between the EDM-180 and the raw LEAP01 PM₁₀ concentrations for the correction period of May 24 to June 30, 2024. The EDM-180 produced much higher hourly PM₁₀ values compared to the raw LEAP01 PM₁₀ values, as shown in Fig. 6. The EDM-180 measured average PM₁₀ concentrations of $21.7 \pm 18.9 \mu\text{g m}^{-3}$ during that period, while the raw LEAP01 reported on average PM₁₀ concentrations of $11.92 \pm 10.82 \mu\text{g m}^{-3}$. EDM-180 PM₁₀ concentrations were on average 2.9 times higher (average difference of $9.81 \pm 19.0 \mu\text{g m}^{-3}$) than those from LEAP01. This poor agreement between the reference instrument and the Clarity sensor is well documented for PM₁₀. Studies demonstrated that the Clarity or the PMS5003 unit underestimates PM₁₀ values (Ramiro et al., 2019; Liu et al., 2022). Liu et al. (2022) found that the Clarity sensor did not match the PM₁₀ measurements produced by the reference unit, similar to the findings of this work. Comparison between the raw LEAP01 PM₁₀ and EDM-180 produced an R² value of 0.08, an RMSE of $10.4 \mu\text{g m}^{-3}$, an MAE of $7.5 \mu\text{g m}^{-3}$, and a slope of 0.2. A linear regression between the two did not show signs of improvement, as the R² value remained low (R² of 0.08), with high RMSE and MAE values (33.3 and $23.7 \mu\text{g m}^{-3}$, respectively), although the slope did improve to 1. 370 Incorporating T and RH into the regression slightly improved it, but not to a usable degree, as R² remained low (R² was 0.24), and high RMSE and MAE values (65.4 and $47.1 \mu\text{g m}^{-3}$, respectively) were reported. Overall, all attempts to correct the PM₁₀ values were unsuccessful. This comes as no surprise, as previous studies have found that the Clarity sensor or the PMS5003 did not respond to variations in PM₁₀ concentrations, regardless of high or low PM₁₀ concentrations, producing very high uncertainties, with a combination of bias and noise (Demanege et al., 2021; Molina Rueda et al., 2023).



375 **Figure 6: Comparison of hourly averaged PM₁₀ values between EDM-180 and raw LEAP01 during May – Jun 2024. (A) Time series with EDM-180 (red) and LEAP01 raw (blue), as well as (B) a box plot between EDM-180 to the raw LEAP01 values.**

380 Based on the comparison provided above, moving forward, LEAP units were calibrated for PM_{2.5} based on TTU calibration (presented in Eq. 1), while corrections of PM₁ were based on Eq. 3. Since only two official reference units are available in the region to monitor PM_{2.5} (EDM-180 and TCEQ BAM-1022), the comparison could only focus on PM_{2.5} concentrations.

3.3 Comparisons of PM_{2.5} concentrations of LEAP with Reference Instruments at collocated locations over long periods

385 Since there are two reference units at two locations in this area, two long-term comparisons were made for PM_{2.5} concentrations between LEAP units to reference units at these collocated sites. In AEROS, the EDM-180 was collocated with three LEAP units (LEAP01, LEAP41, and LEAP42), that were less than 30 m from the EDM-180 and less than a meter from each other (see image in Fig. 1A). Another collocated site was the TCEQ site, where LEAP02 was collocated (3 m apart) with the TCEQ BAM-1022 unit (Fig. 1B). All comparisons were made from July 2, 2024, until February 28, 2025, when all units became active at these collocated sites.

390

3.3.1 Comparison made at the AEROS site

At AEROS, LEAP01 had 5829 overlapping hours with the EDM-180, while LEAP41 and LEAP42 had 5805 and 5804 overlapping hours (respectively). Fluctuation of PM_{2.5} concentrations as measured by each of the LEAP units (for raw and calibrated values) as well as hourly PM_{2.5} concentrations measured by the EDM-180 presented in Fig. 7A. Overall, during the period examined (July - February), hourly PM_{2.5} concentrations from the EDM-180 ranged from 0.37 to 104.3 µg m⁻³, while raw PM_{2.5} concentrations measured by LEAP01 ranged from 0 µg m⁻³ to 54.6 µg m⁻³, and from 1.7 µg m⁻³ to 101.9 µg m⁻³ for the calibrated values. LEAP41 PM_{2.5} concentrations ranged from 0 µg m⁻³ to 53.1 µg m⁻³ for the raw values and from 1.6 µg m⁻³ to 101.1 µg m⁻³ for the calibrated values, while LEAP42 raw PM_{2.5} concentrations ranged from 0 to 49.8 µg m⁻³, and the calibrated values ranged from 2.0 to 103.1 µg m⁻³. Box-and-whisker plots were used to compare the distribution of hourly



400 $PM_{2.5}$ concentrations of the EDM-180 to each of the three LEAP units on AEROS, for both raw and calibrated (shown in Fig. 7B). The EDM-180 hourly $PM_{2.5}$ average value was $7.7 \pm 5.2 \mu g m^{-3}$, while the LEAP01 raw average values were $6.9 \pm 7.5 \mu g m^{-3}$ and $8.1 \pm 5.0 \mu g m^{-3}$ for the calibrated values. LEAP41 average raw values were $7.7 \pm 7.9 \mu g m^{-3}$ and $8.5 \pm 5.1 \mu g m^{-3}$ for the calibrated values, while LEAP42 average values were $7.8 \pm 7.4 \mu g m^{-3}$ for raw and $8.6 \pm 5.0 \mu g m^{-3}$ for the calibrated values. Observations of the box-and-whisker plots show that the LEAP raw values did not capture many high $PM_{2.5}$ values as
405 those detected by the EDM-180 or by the corrected LEAP values. Also, the raw values had a wider value range than those of the EDM-180 and calibrated LEAP units.

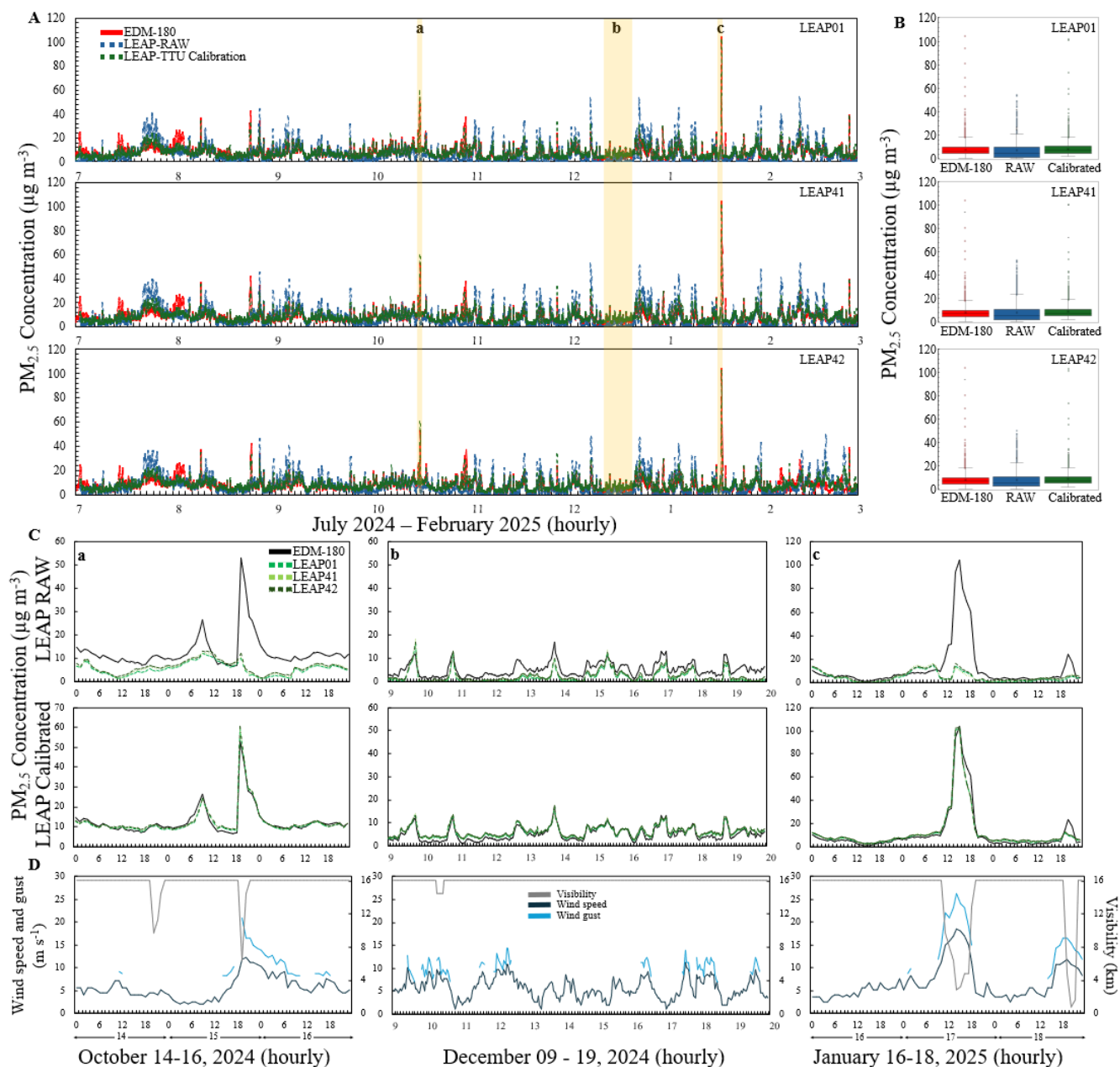
To get a better understanding of the efficiency of the correction of the LEAP units and how it improves the raw values, observations of three events (high and low PM events) were made (Fig. 7C). Observation of the meteorological conditions
410 measured by the ASOS station during these events were made to get a better understanding of the cause of these high PM (Fig. 7D). Two events with high PM concentrations that were caused by dust events were selected (October 15, 2024, and January 17, 2025). The identification of dust events was based on the increase in wind speed and wind gust, with a reduction in visibility with the increase of $PM_{2.5}$ concentrations. Dust event identification was based on the method presented in previous studies for this region (Kelley and Ardon-Dryer, 2021; Ardon-Dryer and Kelley, 2022; Robinson and Ardon-Dryer, 2024; Robinson et
415 al., 2024). In addition, we wanted to examine several days with low PM concentrations to examine the behavior of the correction developed during clean days. December 9 - 19, 2024, fit the criteria as these were 10 days with low wind speed and wind gust, high visibility and low PM concentrations (EDM-180 reported hourly $PM_{2.5}$ concentrations $\leq 17.5 \mu g m^{-3}$ throughout that period).

420 The first event examined was the dust event on October 15, 2024. Observations of hourly $PM_{2.5}$ concentrations from October 14-16, 2024, for both raw and corrected for the three LEAP units on AEROS are presented in Fig. 7C, while the meteorological conditions during these days are presented in Fig. 7D. The dust event took place at 19:00 on October 15, 2024, and lasted for only one hour. During this event, the wind speed increased to $11.8 m s^{-1}$, wind gusts peaked at $21.1 m s^{-1}$, while visibility reduced to 6.4 km, and a BLDU (BLowing DUst) was reported in the ASOS weather code. The EDM-180 measured hourly
425 concentrations of $53.4 \pm 31.7 \mu g m^{-3}$, while the raw $PM_{2.5}$ concentrations from the three LEAP units did not detect this dust, and hourly $PM_{2.5}$ concentrations were below $13 \mu g m^{-3}$. The corrected LEAP hourly $PM_{2.5}$ concentrations were able to detect this dust event, and concentrations ranged from 59.4 to $60.5 \mu g m^{-3}$. Even the hours before and after this dust event seem to overlap nicely with the corrected LEAP values. Comparison of the hourly $PM_{2.5}$ concentrations measured during these 72 hours between the EDM-180 to each of the corrected LEAP units resulted in high correlation values ($R^2 \geq 0.97$), while the raw
430 values had very low correlation values ($R^2 \leq 0.1$). Observations of the difference between the hourly concentrations measured by the EDM-180 to those of the calibrated values for these 72 hours were, on average, $1.0 \mu g m^{-3}$ for each of the three calibrated LEAP units, but the EDM-180 values were, on average, $6.8 \mu g m^{-3}$ higher than those of the raw hourly $PM_{2.5}$ concentrations.



The 10 clean days were next to be examined. During these 264 hours, the EDM-180 hourly $PM_{2.5}$ concentrations ranged from 1.2 to $17.2 \mu\text{g m}^{-3}$. The LEAP raw values from the three units (LEAP01, LEAP41, and LEAP42) ranged from 0 up to $18.4 \mu\text{g m}^{-3}$, while the corrected hourly $PM_{2.5}$ concentrations ranged from 2.8 up to $17.7 \mu\text{g m}^{-3}$. When we examined all these 264 hours, we noticed that the calibrated hourly $PM_{2.5}$ concentrations were on average 0.9 to $1.3 \mu\text{g m}^{-3}$ higher than the EDM-180 hourly $PM_{2.5}$ concentrations. The raw values were on average 2.7 to $3.4 \mu\text{g m}^{-3}$ lower than the EDM-180 hourly $PM_{2.5}$ concentrations. Although there were times of strong winds during these days, none resulted in dust particles as visibility remained high (16.1 km) for most of the duration, and the $PM_{2.5}$ concentrations remained low. There were some small fluctuations in the PM values, and the corrected $PM_{2.5}$ values seem to follow these fluctuations also observed by the EDM-180. This clean period highlights the fact that many of the raw LEAP hourly $PM_{2.5}$ concentrations seem to underestimate the EDM-180 hourly $PM_{2.5}$ concentrations, while most of the corrected LEAP $PM_{2.5}$ concentrations measured slightly higher hourly $PM_{2.5}$ concentrations, but that was on average not more than $1.3 \mu\text{g m}^{-3}$. Comparison of the hourly $PM_{2.5}$ concentrations measured during these hours between the EDM-180 to each of the corrected LEAP units resulted in high correlation values ($R^2 \geq 0.96$), while the raw values had lower correlation values ($R^2 \leq 0.7$).

The last date with an event was the dust event on January 17, 2025. Observations of hourly $PM_{2.5}$ concentrations from January 16-18, 2025, for both raw and corrected for the three LEAP units on AEROS presented in Fig. 7C, while the meteorological conditions during these days presented in Fig. 7D. The dust event started at 11:50 LT when visibility reduced to 9.7 km and lasted until 17:50 LT when visibility went back > 10 km (BLDU was reported in the ASOS weather code). During this time, the lowest visibility reported by ASOS was 2.8 km (at 14:45 LT), the highest wind speed and wind gust measured during this dust event were 18.5 and 26.2 m s^{-1} , respectively. The high hourly $PM_{2.5}$ concentration reported by the EDM-180 on January 17, 2025, at 15:00 LT, was $104.3 \pm 19 \mu\text{g m}^{-3}$. At the same hour, LEAP raw $PM_{2.5}$ concentrations ranged from $9.8 \mu\text{g m}^{-3}$ (LEAP41) up to $14.1 \mu\text{g m}^{-3}$ (LEAP42) while the corrected $PM_{2.5}$ concentrations ranged from 101.1 up to $103.1 \mu\text{g m}^{-3}$. As was observed for the previous dust event, the raw LEAP values did not detect the dust particles, while the corrected LEAP $PM_{2.5}$ values were able to detect the dust, and even at a similar range to the measurements made by the EDM-180. Throughout the 72 hours examined, we noticed that the corrected $PM_{2.5}$ concentrations were on average 2.3 to $2.7 \mu\text{g m}^{-3}$ higher than those measured by the EDM-180. Comparison of the hourly $PM_{2.5}$ concentrations measured during these 72 hours between the EDM-180 to each of the corrected LEAP units resulted in high correlation values ($R^2 \geq 0.97$), while the raw values had much lower correlation values ($R^2 \leq 0.23$). It should be noted that the second reduction of visibility on January 18, 2025, between 19:00 to 21:00 LT was due to a snowfall event and not dust.



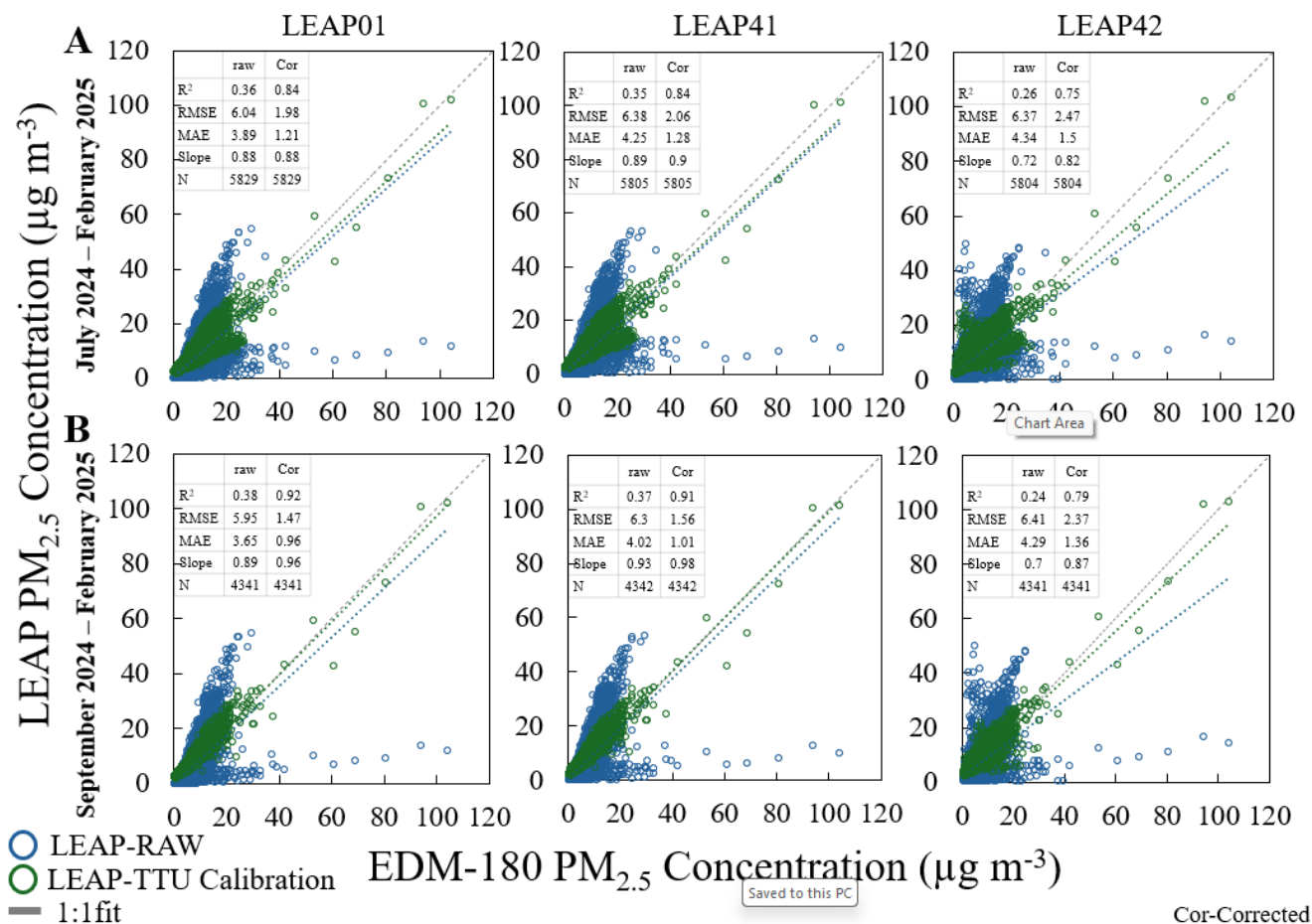
465 **Figure 7: Comparison of PM_{2.5} concentrations from LEAP, raw (blue) and calibrated (green), with reference units EDM-180 at AEROS (in red) for time series plots from July 1, 2024, to Feb 28, 2025. Each plot for a different LEAP unit (A). Box-and-whisker plots comparing the LEAP (raw and calibrated values) with collocated reference units (B). Example of three times of the time series plots of three events (a) October 15 2024, dust event, (b) 10 days of clean days from December 9 to 19 2024 and (c) a dust event on January 17 2025, for each of the LEAP units (raw and calibrated values) with the EDM-180 (C) and meteorological conditions during each of these three events (D).**

470

Based on Fig. 7C, it seems that the three collocated LEAP units (LEAP01, LEAP41, and LEAP42) behave very similarly to one another. Comparison between these three LEAP units, for the entire eight-month period, resulted in $R^2 \geq 0.99$. Although



it seems that there is a good agreement between the corrected LEAP units to the EDM-180 (Fig 7), we wonder if the entire eight-month period examined (> 5000 hours) would also have a good agreement. A comparison between each of the LEAP units to EDM-180 was made. The R^2 values between the EDM-180 and the raw LEAP $PM_{2.5}$ values were 0.36, 0.35, and 0.26, for LEAP01, LEAP41, and LEAP42, respectively. While the R^2 values between EDM-180 and the calibrated LEAP $PM_{2.5}$ values were much higher, with R^2 of 0.86, 0.84, and 0.75 for LEAP01, LEAP41, and LEAP42, respectively. An improvement in RMSE was also observed. The raw values had RMSE values of 6.0, 6.4, and 6.4 $\mu\text{g m}^{-3}$ compared to 2.0, 2.1, and 2.5 $\mu\text{g m}^{-3}$ for the calibrated LEAP01, LEAP41, and LEAP42, respectively. MAE values also reduced from 3.9, 4.3, and 4.3 $\mu\text{g m}^{-3}$ for the raw (for LEAP01, LEAP41, and LEAP42, respectively), to 1.2, 1.3, and 1.5 $\mu\text{g m}^{-3}$ for the calibrated (for LEAP01, LEAP41, and LEAP42, respectively). The slope did not demonstrate significant improvement, the raw LEAP slopes were 0.88, 0.89, and 0.72, compared to 0.88, 0.9, and 0.82 for the calibrated slope for LEAP01, LEAP41, and LEAP42, respectively (Fig. 8A). A close look at the time series (Fig. 7A), along with the deviation from the 1:1 line and the relatively lower R^2 values expected from the corrected LEAP units at AEROS (Fig. 8A), at least for LEAP01 which was used for calibration, leads to further examination of the data. It was noticed that there were several days in July and August when the reference unit detected higher $PM_{2.5}$ concentrations than the LEAP units. To examine that aspect, a comparison between the EDM-180 and LEAP01, since it was used to develop calibration, for each month was performed (Fig. S2). Each month examined produced a good correlation for $PM_{2.5}$ concentrations, with R^2 values > 0.9, except for July and August, which had lower R^2 values. Similar findings were also observed for LEAP41 and LEAP42 (data not shown). We were puzzled by this behavior as we could not find an explanation for what caused the July and August deviations. We examined the changes of internal sensor T and RH during these months compared to the other months, but it did not seem to be off (Fig. S3). We also examined additional meteorological conditions during these months measured by the ASOS unit, including T and RH, dew point temperature, wind speed, and visibility (Fig. S3), but it did not seem that July and August had different conditions compared to the other months. We wondered if the removal of these two months from the comparison would improve the correlation between the reference unit and the LEAP units. Removing these two months (July and August) left > 4341 overlapping hours between the three LEAP units in AEROS. R^2 values for these comparisons improved from an R^2 of 0.75 to 0.84 when July and August were included, up to an R^2 of 0.79 to 0.92 without July and August (Fig. 8B). A significant improvement was also observed with the reduction of RMSE and MAE values, as well as with the slope values, which were closer to a 1-to-1 line. A stronger improvement was seen for LEAP01 and LEAP41 compared to LEAP42, as its improvement was slightly less significant. Future work should be taken to understand if specific events led to the difference between the units (not maintaining $R^2 > 0.95$) and what led to July and August having an offset in the $PM_{2.5}$ concentrations that led to their low correlations.



510 **Figure 8: Comparison of PM_{2.5} hourly concentrations between LEAP raw (blue) and LEAP calibrated (green) to the EDM-180 for July to February (A) and for September to February (B). Statistics of each comparison are provided in the Table in each scatter plot. The dashed line represents the best fit between the EDM-180 to the LEAP, and the gray sash line represents the 1:1 line.**

3.3.2 Comparison made at the TCEQ site

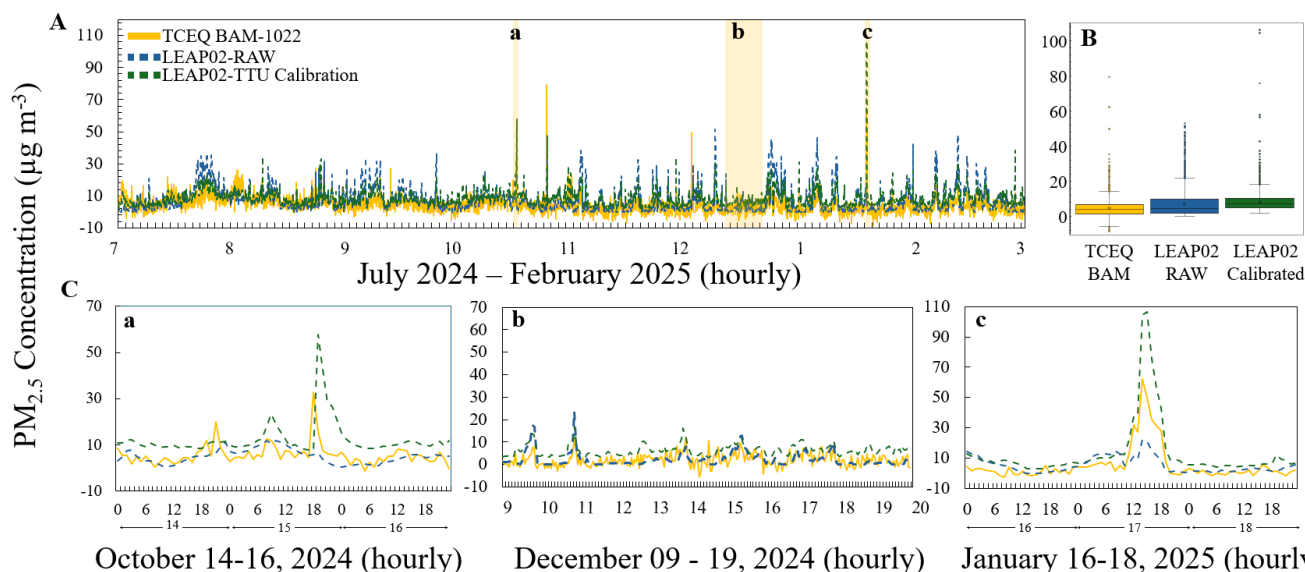
The second reference unit is the one operated by TCEQ that hosts a BAM-1022 unit. PM_{2.5} concentrations measured by LEAP02 were compared to the TCEQ unit. LEAP02 had 5800 overlapping hours of measurements with the BAM-1022 unit. For the measured period, PM_{2.5} concentrations from the BAM-1022 unit ranged from -8.2 to 79.3 μg m⁻³. 12.5% of the values of the BAM-1022 were < 0 μg m⁻³. LEAP02 PM_{2.5} concentrations ranged from 0 to 51.6 μg m⁻³ for the raw values and from 1.8 to 106.3 μg m⁻³ for the calibrated values. Overall, there were 5800 hours overlapping with PM_{2.5} measurements of both BAM-1022 and LEAP02 units. During that time, the average hourly PM_{2.5} concentration by the BAM-1022 was 4.4 ± 4.6 μg m⁻³, while the average PM_{2.5} concentrations from LEAP02 reported were 6.95 ± 7.3 and 8.2 ± 4.96 μg m⁻³ for the raw and calibrated values, respectively. The time series plot (Fig. 9A) as well as the box-and-whisker plot comparing the BAM-1022

520



unit to LEAP02 (Fig. 9B) show that BAM-1022 measured much lower concentrations overall compared to the raw and calibrated LEAP02, found with other similar collocated BAM-1020/BAM-1022 series units to other FRM/FEM units (Long et al., 2023).

- 525 All three events: October 15, 2024, dust event, 10 days of clean days, December 9 to 19, 2024, and dust event on January 17, 2025, were examined (Fig. 9C). These events show mixed results, with some showing good agreement between the corrected LEAP02 and the BAM-1022, while others show no agreement at all. For the first dust event of October 15, 2024, at the peak of the dust, the BAM-1022 detected hourly $\text{PM}_{2.5}$ concentrations of $32.8 \mu\text{g m}^{-3}$ (at 18:00 LT) while the corrected LEAP02 detected $57.9 \mu\text{g m}^{-3}$ (at 19:00 LT). This disagreement with the time of peak seems like an issue only for this specific event.
- 530 Both the corrected LEAP02 and the BAM-1022 detected the dust peak of January 17, 2025, at the same time, but the difference in concentration was significant. While the BAM-1022 reported hourly $\text{PM}_{2.5}$ concentrations of $62.2 \mu\text{g m}^{-3}$, the corrected LEAP02 detected concentrations of $106.3 \mu\text{g m}^{-3}$. It should be noted that the EDM-180, $\text{PM}_{2.5}$ concentration was $104.3 \pm 19 \mu\text{g m}^{-3}$ at the same time.
- 535 When we examined the correlations between these hours, we found that for the October case, the BAM-1022 had a low correlation value (R^2 of 0.07) to LEAP02, but for the 72 hours examined during January, this correlation value was high (R^2 was 0.93). A close look at the difference between the $\text{PM}_{2.5}$ concentrations showed that for 96% of the 72 hours in October, and 99% of the hours in January, the corrected LEAP02 values were higher than that BAM-1022. As for the raw LEAP02 values, ~50% of the hourly $\text{PM}_{2.5}$ concentrations were higher than the concentrations measured by the BAM-1022. Similar
- 540 findings were also seen for the clean days of December 9 to 19, 2024. About 50% of the LEAP02 raw hourly $\text{PM}_{2.5}$ concentrations were higher than the concentrations measured by the BAM-1022, and 95% of the corrected LEAP02 values were higher than the concentrations measured by the BAM-1022. Even the comparison of the hourly $\text{PM}_{2.5}$ concentrations measured during the 264 hours compared between BAM-1022 and LEAP02 was low ($R^2 \leq 0.3$ for both raw and corrected LEAP02 values).



545 **Figure 9: Comparison of PM_{2.5} concentrations from LEAP02, raw (blue) and calibrated (green), with reference units BAM-1022 at TCEQ site (in orange) for time series plots from July 1, 2024, to Feb 28, 2025. Box-and-whisker plots comparing the LEAP (raw and calibrated values) with collocated reference units (B). (C) Example of three times of the time series plots of three events (a) October 15, 2024, dust event, (b) 10 days of clean days from December 9 to 19, 2024, and (c) a dust event on January 17, 2025.**

550

Since these examples had mixed results, a full comparison between the BAM-1022 and LEAP02 was made (Fig. S4). This comparison did not produce a good agreement, as those reported for AEROS. The R^2 value between the BAM-1022 and LEAP02 raw measurements was 0.22, while the corrected LEAP02 measurements produced a slight increase in R^2 values, but still low (R^2 of 0.34). RMSE was $6.5 \mu\text{g m}^{-3}$ for raw LEAP02 and $4.0 \mu\text{g m}^{-3}$ for the corrected LEAP02. MAE value slightly improved from $4.6 \mu\text{g m}^{-3}$ to $2.8 \mu\text{g m}^{-3}$ (for raw vs. calibrated, respectively), yet both RMSE and MAE values were still significantly higher than for the comparison made in AEROS. Overall, neither the raw nor calibrated data from LEAP02 provided a good correlation with the data from the TCEQ BAM-1022. Even when the measurements from July and August were removed (Fig. S4), the correlations between the units remain low (R^2 was 0.43, RMSE was $3.9 \mu\text{g m}^{-3}$, MAE was 2.68, while the slope was 0.81).

560

Since the distance between AEROS and TCEQ is only 8.2 km, we wonder if a comparison between the two sites reference units could help us understand what led to the low comparison (LEAP02 TO TCEQ BAM-1022). Low correlations values were found between the BAM-1022 and EDM-180 (R^2 was 0.41, RMSE was $4.0 \mu\text{g m}^{-3}$, MAE was $2.7 \mu\text{g m}^{-3}$ while the slope was 0.81, based on 4321 hours of comparison). However, the EDM-180 had high comparison to the corrected LEAP02 unit with R^2 of 0.89, RMSE and MAE of 1.7 and $1.1 \mu\text{g m}^{-3}$ and a slope of 0.95, (based on 4341 hours of comparison). Even the three corrected LEAP units in AEROS (LEAP01, LEAP41, and LEAP42) had a better agreement with the corrected LEAP02 (R^2 ranged from 0.8 for LEAP42 up to 0.94 for LEAP01 and LEAP41; for 4341 comparison hours). It should be noted that even when July and August were removed from the analysis, similar findings were retrieved. We noticed that overall, hourly

565



PM_{2.5} from the corrected LEAP02 (82.9% of the 6588 hours examined) were higher than those measured by the BAM-1022. Even the EDM-180 had higher hourly PM_{2.5} concentrations than the BAM-1022 (80.7% of the 6592 hours examined). We speculate that the numerous negative values produced by the BAM-1022 unit, coupled with the calibration for LEAP02 being developed based on the EDM-180, led to this low comparison. It should be noted that we did not have any control over the BAM-1022 unit, as it was operated and calibrated by the TCEQ. We speculated that the lowered regression values resulted from the subzero PM_{2.5} measurements, as BAM-1022 can measure concentrations down to -15 µg m⁻³ (Met One, 2025). During the examined period, there were 688 hours when the BAM-1022 unit reported PM_{2.5} concentrations < 0 µg m⁻³. The PM_{2.5} concentrations from the calibrated LEAP02 of these hours ranged from 1.9 up to 15.6 µg m⁻³. Additional studies reported negative PM_{2.5} concentration values from the BAM units (Khreis et al., 2022). Some studies converted the negative values to 0 µg m⁻³, while others used a lower limit of detection threshold for the PM_{2.5} concentrations (Magi et al., 2020; Khreis et al., 2022). Multiple attempts were made including removal of all the reported negative values, converting the negative values to 0 µg m⁻³ as suggested by Khreis et al. (2022), as well as using a limit of detection threshold (2.4 µg m⁻³; based on Magi et al., 2019). Yet none of these attempts improved the regression between LEAP02 to the TCEQ BAM-1022 unit; R² values remained below 0.4. To examine the BAM-1022 negative values in depth, we check all the minimum daily values reported by TCEQ since the site became operational (on August 13, 2016). From August 13, 2016, to July 11, 2018, the site hosted a TEOM unit. On July 11, 2018, the unit was replaced with the BAM-1022. None of the 667 days when the TEOM was operated had negative hourly PM_{2.5} concentrations. Out of the 2278 days examined since the BAM-1022 became operational (July 11, 2018, to December 31, 2024), more than half (53.2%) had negative PM_{2.5} concentrations daily minimum. These findings highlight the need to continue examining the TCEQ site in order to understand the behavior of the BAM-1022 unit.

Since LEAP02 behaves in a similar manner to the other LEAP units in AEROS, as well as to EDM-180, we speculated that the issue is with the BAM-1022 unit and not with LEAP02. Good agreement between corrected Clarity PM_{2.5} values and reference instruments over longer periods was also found in previous studies (Zaidan et al., 2020; Raheja et al., 2023; Njeru et al., 2024). Supporting the overall findings from this study, at least for the AEROS site.

4 Summary

This study focused on examining the performance of four Clarity Node S units at two sites with reference units (EDM-180 in AEROS and BAM-1022 at TCEQ site). At first all four sensors were compared to each other (1881 hours) for all three PM sizes, and a good intercomparison agreement was found with high R² and low RMSE and MAE values. This allowed for the viability of developing a calibration with one sensor and applying it to the other sensors in the network.

Next different calibrations test was performed to evaluate the performance Clarity Node S units. 12 different regressions were applied to correct the raw LEAP01 PM_{2.5} values, with the best performing regression using LEAP internal T and RH



measurements, along with the PM_{10} values measured by EDM-180. This regression produced the highest R^2 (R^2 of 0.93) and lowest RMSE and MAE (1.5 and $0.9 \mu\text{g m}^{-3}$, respectively). Four different regressions were tested to improve PM_1 comparisons. The best regression model used the LEAP internal T and RH measurements, along with EDM-180 PM_{10} values. This regression produced an R^2 of 0.96, an RMSE of $0.9 \mu\text{g m}^{-3}$, an MAE of $0.55 \mu\text{g m}^{-3}$, and a slope of 1, an improvement compared to raw
605 LEAP values. An attempt was made to improve the LEAP PM_{10} , yet all tests had very low R^2 and high RMSE and MAE values, ultimately making us conclude that PM_{10} readings from LEAP were unreliable.

The calibrated values were implemented on each of the four LEAP units and each of the unit (raw and calibrated values) were then compared to collocated (for eight months) to a reference unit. Three LEAP units (LEAP01, LEAP41 and LEAP42) were
610 compared to EDM-180 in AEROS while LEAP02 was collocated to the BAM-1022 at the TCEQ site. The collocated calibrated LEAP units in AEROS tested well with the EDM-180 unit, apart from a problematic July and August comparison. The comparison produced high R^2 and low RMSE and MAE values (from September 1, 2024, to February 28, 2025). The collocated BAM-1022 and LEAP02 unit at the TCEQ site did not have as good a comparison, with low R^2 and high RMSE and MAE values. The inconsistency in finding at the TCEQ site will require further examination to determine the cause of these
615 differences.

Data availability

Automatic surface observation systems (ASOS) are available from the Iowa University Mesonet (Iowa State Mesonet, 2025). PM measurements from BAM-1022 were retrieved from the Texas Commission on Environmental Quality (TCEQ, 2025). WTM data were provided by the WTM team (WTM, 2025). Real-time data of LEAP sensors available on the Lubbock
620 Compact website (Lubbock Compact, 2025). All measurements are available from the authors upon request.

Author contributions

JG and KAD were involved in the deployment of sensors, data analysis, and calibration development. KAD designed the study and coordinated the different aspects of the manuscript. All authors were actively involved in interpreting the results and in discussions on the manuscript.

625 Competing interests

The contact author has declared that none of the authors has any competing interests.



Acknowledgment

This research, “Lubbock Environmental Action Plan (LEAP) for Communities,” was funded by the EPA (grant # 02F28601). The authors would like to thank Mr. Matthew Asel from the National Wind Institute at Texas Tech University for providing us with the WTM data.

References

- Alizadeh-Choobari, O., and M. Gharaylou, 2017: Aerosol impacts on radiative and microphysical properties of clouds and precipitation formation. *Atmospheric Res.*, **185**, 53–64, <https://doi.org/10.1016/j.atmosres.2016.10.021>.
- Analitis, A., B. Barratt, D. Green, A. Beddows, E. Samoli, J. Schwartz, and K. Katsouyanni, 2020: Prediction of PM_{2.5} concentrations at the locations of monitoring sites measuring PM₁₀ and NO_x, using generalized additive models and machine learning methods: A case study in London. *Atmos. Environ.*, **240**, 117757, <https://doi.org/10.1016/j.atmosenv.2020.117757>.
- AQ-SPEC, 2018a: Field Evaluation Clarity Node PM Sensor. https://www.aqmd.gov/docs/default-source/aq-spec/laboratory-evaluations/clarity-node---lab-evaluation.pdf?sfvrsn=9e55f261_25
- AQ-SPEC, 2018b: Laboratory Evaluation Clarity Node PM Sensor. https://www.aqmd.gov/docs/default-source/aq-spec/laboratory-evaluations/clarity-node---lab-evaluation.pdf?sfvrsn=9e55f261_25
- Ardon-Dryer, K., and M. C. Kelley, 2022: Particle size distribution and particulate matter concentrations during synoptic and convective dust events in West Texas. *Atmospheric Chem. Phys.*, **22**, 9161–9173, <https://doi.org/10.5194/acp-22-9161-2022>.
- Ardon-Dryer, K., and T. Aziz, 2025: Times Matter, the Impact of Convective Dust Events on Air Quality in the Greater Phoenix Area, Arizona. *GeoHealth*, **9**, e2024GH001209, <https://doi.org/10.1029/2024GH001209>.
- Ardon-Dryer, K., Y. Dryer, J. N. Williams, and N. Moghimi, 2020: Measurements of PM_{2.5} with PurpleAir under atmospheric conditions. *Atmospheric Meas. Tech.*, **13**, 5441–5458, <https://doi.org/10.5194/amt-13-5441-2020>.
- Ardon-Dryer, V. Chmielewski, E. C. Bruning, and X. Xueting, 2022a: Changes of electric field, aerosol, and wind covariance in different blowing dust days in West Texas. *Aeolian Res.*, **54**, 100762, <https://doi.org/10.1016/j.aeolia.2021.100762>.
- Ardon-Dryer, M. C. Kelley, X. Xueting, and Y. Dryer, 2022b: The Aerosol Research Observation Station (AEROS). *Atmospheric Meas. Tech.*, **15**, 2345–2360, <https://doi.org/10.5194/amt-15-2345-2022>.
- Ardon-Dryer, K., K. R. Clifford, and J. L. Hand, 2023: Dust Under the Radar: Rethinking How to Evaluate the Impacts of Dust Events on Air Quality in the United States. *GeoHealth*, **7**, e2023GH000953, <https://doi.org/10.1029/2023GH000953>.
- Attey-Yeboah, P., and Coauthors, 2025: Utility of low-cost sensor measurement for predicting ambient PM_{2.5} concentrations: evidence from a monitoring network in Accra, Ghana. *Environ. Sci. Atmospheres*, **5**, 517–529, <https://doi.org/10.1039/d4ea00140k>.



- Bangert, M., and Coauthors, 2012: Saharan dust event impacts on cloud formation and radiation over Western Europe. *Atmospheric Chem. Phys.*, **12**, 4045–4063, <https://doi.org/10.5194/acp-12-4045-2012>.
- 660
- Barkjohn, K. K., B. Gantt, and A. L. Clements, 2021a: Development and application of a United States-wide correction for PM_{2.5} data collected with the PurpleAir sensor. *Atmospheric Meas. Tech.*, **14**, 4617–4637, <https://doi.org/10.5194/amt-14-4617-2021>.
- Byrne, R., J. C. Wenger, and S. Hellebust, 2024: Spatial analysis of PM_{2.5} using a concentration similarity index applied to air quality sensor networks. *Atmospheric Meas. Tech.*, **17**, 5129–5146, <https://doi.org/10.5194/amt-17-5129-2024>.
- 665
- Chakrabarti, B., P. M. Fine, R. Delfino, and C. Sioutas, 2004: Performance evaluation of the active-flow personal DataRAM PM_{2.5} mass monitor (Thermo Anderson pDR-1200) designed for continuous personal exposure measurements. *Atmos. Environ.*, **38**, 3329–3340, <https://doi.org/10.1016/j.atmosenv.2004.03.007>.
- Chueinta, W., and P. K. Hopke, 2001: Beta Gauge for Aerosol Mass Measurement. *Aerosol Sci. Technol.*, **35**, 840–843, <https://doi.org/10.1080/027868201753227398>.
- 670
- Clarity, 2023: Clarity Node-S: PM & NO₂ Air Quality Sensor. *Clarity Node S*. Accessed 9 November 2023, <https://www.clarity.io/products/clarity-node-s>.
- Clements, A., and R. Vanderpool, 2019: EPA Tools and Resources Webinar FRMs/FEMs and Sensors: Complementary Approaches for Determining Ambient Air Quality. 27. https://www.epa.gov/sites/default/files/2019-12/documents/frm-fem_and_air_sensors_dec_2019_webinar_slides_508_compliant.pdf
- 675
- Crilley, L. R., M. Shaw, R. Pound, L. J. Kramer, R. Price, S. Young, A. C. Lewis, and F. D. Pope, 2018: Evaluation of a low-cost optical particle counter (Alphasense OPC-N2) for ambient air monitoring. *Atmospheric Meas. Tech.*, **11**, 709–720, <https://doi.org/10.5194/amt-11-709-2018>.
- Delgado-Saborit, J. M., 2012: Use of real-time sensors to characterise human exposures to combustion related pollutants. *J. Environ. Monit.*, **14**, 1824–1837, <https://doi.org/10.1039/C2EM10996D>.
- 680
- Demanege, I., I. Mujan, B. C. Singer, A. S. Anđelković, F. Babich, and D. Licina, 2021: Performance assessment of low-cost environmental monitors and single sensors under variable indoor air quality and thermal conditions. *Build. Environ.*, **187**, 107415, <https://doi.org/10.1016/j.buildenv.2020.107415>.
- Eatough, D. J., N. L. Eatough, F. Obeidi, Y. Pang, W. Modey, and R. Long, 2001: Continuous Determination of PM_{2.5} Mass, Including Semi-Volatile Species. *Aerosol Sci. Technol.*, **34**, 1–8, <https://doi.org/10.1080/02786820121229>.
- 685
- Eisner, A. D., and R. W. Wiener, 2002: Discussion and Evaluation of the Volatility Test for Equivalency of Other Methods to the Federal Reference Method for Fine Particulate Matter. *Aerosol Sci. Technol.*, **36**, 433–440, <https://doi.org/10.1080/027868202753571250>.
- EPA, 2024: Reconsideration of the National Ambient Air Quality Standards for Particulate Matter; Correction. *Fed. Regist.* Accessed 7 April 2025, <https://www.federalregister.gov/documents/2024/12/19/2024-29223/reconsideration-of-the-national-ambient-air-quality-standards-for-particulate-matter-correction>.
- 690



- Escobar-Diaz, F., C. Buitrago, L. Quiñones, F. Grajales, and T. Mejia, 2021: Evaluation of particulate matter microsensors to build the low-cost sensors collaborative network of Bogotá. *2021 Congreso Colombiano y Conferencia Internacional de Calidad de Aire y Salud Pública (CASAP)*, 2021 Congreso Colombiano y Conferencia Internacional de Calidad de Aire y Salud Pública (CASAP), 1–5, <https://doi.org/10.1109/CASAP54985.2021.9703377>.
- 695
- Fiore, A. M., V. Naik, and E. M. Leibensperger, 2015: Air Quality and Climate Connections. *J. Air Waste Manag. Assoc.*, **65**, 645–685, <https://doi.org/10.1080/10962247.2015.1040526>.
- Goyal, P., N. Jaiswal, A. Kumar, J. K. Dadoo, and M. Dwarakanath, 2010: Air quality impact assessment of NO_x and PM due to diesel vehicles in Delhi. *Transp. Res. Part Transp. Environ.*, **15**, 298–303, <https://doi.org/10.1016/j.trd.2010.03.002>.
- 700
- Grimm, H., and D. Eatough, 2009: Aerosol Measurement: The Use of Optical Light Scattering for the Determination of Particulate Size Distribution, and Particulate Mass, Including the Semi-Volatile Fraction. *J. Air Waste Manag. Assoc. 1995*, **59**, 101–107, <https://doi.org/10.3155/1047-3289.59.1.101>.
- GRIMM/DURAG, 2020: *Stationary Environmental Dust Measurement Device Environmental Dust Monitor Model EDM 180. EDM180_Manual_2020.pdf*. <https://www.durag.com/en/product-filter-837.htm?productID=EDM%20180>.
- 705
- Hagan, D. H., and J. H. Kroll, 2020: Assessing the accuracy of low-cost optical particle sensors using a physics-based approach. *Atmospheric Meas. Tech.*, **13**, 6343–6355, <https://doi.org/10.5194/amt-13-6343-2020>.
- Huang, W., and Coauthors, 2009: Visibility, air quality and daily mortality in Shanghai, China. *Sci. Total Environ.*, **407**, 3295–3300, <https://doi.org/10.1016/j.scitotenv.2009.02.019>.
- Iowa State Mesonet, 2025: IEM :: Download ASOS/AWOS/METAR Data. Accessed 15 August 2025, https://mesonet.agron.iastate.edu/request/download.phtml?network=TX_ASOS.
- 710
- Jiao, W., and Coauthors, 2016: Community Air Sensor Network (CAIRSENSE) project: evaluation of low-cost sensor performance in a suburban environment in the southeastern United States. *Atmospheric Meas. Tech.*, **9**, 5281–5292, <https://doi.org/10.5194/amt-9-5281-2016>.
- Kampa, M., and E. Castanas, 2008: Human health effects of air pollution. *Environ. Pollut.*, **151**, 362–367, <https://doi.org/10.1016/j.envpol.2007.06.012>.
- 715
- Kelley, M. C., and K. Ardon-Dryer, 2021: Analyzing two decades of dust events on the Southern Great Plains region of West Texas. *Atmospheric Pollut. Res.*, **12**, 101091, <https://doi.org/10.1016/j.apr.2021.101091>.
- Kelley, M. C., M. M. Brown, C. B. Fedler, and K. Ardon-Dryer, 2020: Long-term Measurements of PM_{2.5} Concentrations in Lubbock, Texas. *Aerosol Air Qual. Res.*, **20**, 1306–1318, <https://doi.org/10.4209/aaqr.2019.09.0469>.
- 720
- Khreis, H., J. Johnson, K. Jack, B. Dadashova, and E. S. Park, 2022: Evaluating the Performance of Low-Cost Air Quality Monitors in Dallas, Texas. *Int. J. Environ. Res. Public Health*, **19**, 1647, <https://doi.org/10.3390/ijerph19031647>.
- Lewis, A., and P. Edwards, 2016: Validate personal air-pollution sensors. *Nature*, **535**, 29–31, <https://doi.org/10.1038/535029a>.
- Liu, G., and Coauthors, 2022: Chemical explosion, COVID-19, and environmental justice: Insights from low-cost air quality sensors. *Sci. Total Environ.*, **849**, 157881, <https://doi.org/10.1016/j.scitotenv.2022.157881>.



- 725 Long, R. W., Urbanski ,Shawn P., Lincoln ,Emily, Colón ,Maribel, Kaushik ,Surender, Krug ,Jonathan D., Vanderpool ,Robert W., and M. S. and Landis, 2023: Summary of PM_{2.5} measurement artifacts associated with the Teledyne T640 PM Mass Monitor under controlled chamber experimental conditions using polydisperse ammonium sulfate aerosols and biomass smoke. *J. Air Waste Manag. Assoc.*, **73**, 295–312, <https://doi.org/10.1080/10962247.2023.2171156>.
- Lubbock Compact, 2025: LEAP (Lubbock Environmental Action Plan) Project. *LEAP Proj.* Accessed 21 August 2025,
730 <https://lubbockcompact.com/leap-project/>.
- Magi, B. I., Cupini ,Calvin, Francis ,Jeff, Green ,Megan, and C. and Hauser, 2020: Evaluation of PM_{2.5} measured in an urban setting using a low-cost optical particle counter and a Federal Equivalent Method Beta Attenuation Monitor. *Aerosol Sci. Technol.*, **54**, 147–159, <https://doi.org/10.1080/02786826.2019.1619915>.
- Malm, W. C., J. F. Sisler, D. Huffman, R. A. Eldred, and T. A. Cahill, 1994: Spatial and seasonal trends in particle concentration
735 and optical extinction in the United States. *J. Geophys. Res. Atmospheres*, **99**, 1347–1370, <https://doi.org/10.1029/93JD02916>.
- Megaritis, A. G., C. Fountoukis, P. E. Charalampidis, H. a. C. Denier van der Gon, C. Pilinis, and S. N. Pandis, 2014: Linking climate and air quality over Europe: effects of meteorology on PM_{2.5} concentrations. *Atmospheric Chem. Phys.*, **14**, 10283–10298, <https://doi.org/10.5194/acp-14-10283-2014>.
- 740 Met One, 2019: BAM 1020 Particulate Monitor Operation Manual. <https://metone.com/products/bam-1022/>
- Met One, 2025: BAM-1022 Beta Attenuation Mass Monitor. *Met One Instrum.* Accessed 28 April 2025, <https://metone.com/products/bam-1022/>.
- Mignacca, D., and K. Stubbs, 1999: Effects of Equilibration Temperature on PM₁₀ Concentrations from the TEOM Method in the Lower Fraser Valley. *J. Air Waste Manag. Assoc.*, **49**, 1250–1254,
745 <https://doi.org/10.1080/10473289.1999.10463914>.
- Molina Rueda, E., E. Carter, C. L'Orange, C. Quinn, and J. Volckens, 2023: Size-Resolved Field Performance of Low-Cost Sensors for Particulate Matter Air Pollution. *Environ. Sci. Technol. Lett.*, **10**, 247–253, <https://doi.org/10.1021/acs.estlett.3c00030>.
- Nguyen, P. D. M., N. Martinussen, G. Mallach, G. Ebrahimi, K. Jones, N. Zimmerman, and S. B. Henderson, 2021: Using
750 Low-Cost Sensors to Assess Fine Particulate Matter Infiltration (PM_{2.5}) during a Wildfire Smoke Episode at a Large Inpatient Healthcare Facility. *Int. J. Environ. Res. Public Health*, **18**, 9811, <https://doi.org/10.3390/ijerph18189811>.
- Nobell, S., and Coauthors, 2023: Validation of In-field Calibration for Low-Cost Sensors Measuring Ambient Particulate Matter in Kolkata, India, <https://doi.org/10.26434/chemrxiv-2023-8lhrq-v2>.
- NWS, 2025: NWS Lubbock, TX - Local Climate Data. Accessed 15 August 2025, [https://www.weather.gov/lub/climate-klbb-
755 pcpn](https://www.weather.gov/lub/climate-klbb-pcpn).
- Ouimette, J. R., W. C. Malm, B. A. Schichtel, P. J. Sheridan, E. Andrews, J. A. Ogren, and W. P. Arnott, 2022: Evaluating the PurpleAir monitor as an aerosol light scattering instrument. *Atmospheric Meas. Tech.*, **15**, 655–676, <https://doi.org/10.5194/amt-15-655-2022>.



- Papapostolou, V., H. Zhang, B. J. Feenstra, and A. Polidori, 2017: Development of an environmental chamber for evaluating
760 the performance of low-cost air quality sensors under controlled conditions. *Atmos. Environ.*, **171**, 82–90,
<https://doi.org/10.1016/j.atmosenv.2017.10.003>.
- Patashnick, H., and E. G. Rupperecht, 1991: Continuous PM-10 Measurements Using the Tapered Element Oscillating
Microbalance. *J. Air Waste Manag. Assoc.*, **41**, 1079–1083, <https://doi.org/10.1080/10473289.1991.10466903>.
- PurpleAir, 2023: PurpleAir Classic Air Quality Monitor. *PurpleAir Inc.* Accessed 9 November 2023,
765 <https://www2.purpleair.com/products/purpleair-pa-ii>.
- Raheja, G., and Coauthors, 2023: Low-Cost Sensor Performance Intercomparison, Correction Factor Development, and 2+
Years of Ambient PM_{2.5} Monitoring in Accra, Ghana. *Environ. Sci. Technol.*, **57**, 10708–10720,
<https://doi.org/10.1021/acs.est.2c09264>.
- Ramiro, E. D., B. Artíñano, A. Rubio, I. Figuero, M. Barreiro, and J. Fernández, 2019: Field Assessment of Low-cost
770 Particulate Matter Sensors against Reference Methods. *2019 5th Experiment International Conference (exp.at'19)*,
2019 5th Experiment International Conference (exp.at'19), 444–448, <https://doi.org/10.1109/EXPAT.2019.8876519>.
- Rees, S. L., A. L. Robinson, A. Khlystov, C. O. Stanier, and S. N. Pandis, 2004: Mass balance closure and the Federal Reference
Method for PM_{2.5} in Pittsburgh, Pennsylvania. *Atmos. Environ.*, **38**, 3305–3318,
<https://doi.org/10.1016/j.atmosenv.2004.03.016>.
- 775 Robinson, M. C., K. Schueth, and K. Ardon-Dryer, 2024: Spatial, temporal, and meteorological impact of the 26 February
2023 dust storm: increase in particulate matter concentrations across New Mexico and West Texas. *Atmospheric Chem.*
Phys., **24**, 13733–13750, <https://doi.org/10.5194/acp-24-13733-2024>.
- Roque, N. A., H. Andrews, and A. R. Santos-Lozada, 2025: Identifying air quality monitoring deserts in the United States.
Proc. Natl. Acad. Sci., **122**, e2425310122, <https://doi.org/10.1073/pnas.2425310122>.
- 780 Rovira, J., J. L. Domingo, and M. Schuhmacher, 2020: Air quality, health impacts and burden of disease due to air pollution
(PM₁₀, PM_{2.5}, NO₂ and O₃): Application of AirQ+ model to the Camp de Tarragona County (Catalonia, Spain). *Sci.*
Total Environ., **703**, 135538, <https://doi.org/10.1016/j.scitotenv.2019.135538>.
- Shaughnessy, W. J., M. M. Venigalla, and D. Trump, 2015: Health effects of ambient levels of respirable particulate matter
(PM) on healthy, young-adult population. *Atmos. Environ.*, **123**, 102–111,
785 <https://doi.org/10.1016/j.atmosenv.2015.10.039>.
- Shim, J., S. Park, and D. Song, 2025: Impact of particulate matter (PM₁₀, PM_{2.5}) on global horizontal irradiance and direct
normal irradiance in urban areas. *Build. Environ.*, **271**, 112610, <https://doi.org/10.1016/j.buildenv.2025.112610>.
- Solomon, P. A., D. Crumpler, J. B. Flanagan, R. K. M. Jayanty, E. E. Rickman, and C. E. McDade, 2014: U.S. National PM_{2.5}
Chemical Speciation Monitoring Networks—CSN and IMPROVE: Description of networks. *J. Air Waste Manag.*
790 *Assoc.*, **64**, 1410–1438, <https://doi.org/10.1080/10962247.2014.956904>.
- Soneja, S., C. Chen, J. M. Tielsch, J. Katz, S. L. Zeger, W. Checkley, F. C. Curriero, and P. N. Breyse, 2014: Humidity and
Gravimetric Equivalency Adjustments for Nephelometer-Based Particulate Matter Measurements of Emissions from



- Solid Biomass Fuel Use in Cookstoves. *Int. J. Environ. Res. Public. Health*, **11**, 6400–6416, <https://doi.org/10.3390/ijerph110606400>.
- 795 Spinelle, L., M. Gerboles, M. G. Villani, M. Aleixandre, and F. Bonavitacola, 2015: Field calibration of a cluster of low-cost available sensors for air quality monitoring. Part A: Ozone and nitrogen dioxide. *Sens. Actuators B Chem.*, **215**, 249–257, <https://doi.org/10.1016/j.snb.2015.03.031>.
- Sufleta, A., 2025: Impacts of Lowered PM2.5 NAAQS to Take Shape in 2025 and other NAAQS Related Updates. *ALL4*. Accessed 7 April 2025, <https://www.all4inc.com/4-the-record-articles/impacts-of-lowered-pm2-5-naaqs-to-take-shape-in-2025-and-other-naaqs-related-updates/>.
- 800 TCEQ, 2025: Monthly Summary Report for CAMS 1028. Accessed 15 August 2025, https://www.tceq.texas.gov/cgi-bin/compliance/monops/monthly_summary.pl?cams=1028.
- Valavanidis, A., K. Fiotakis, and T. Vlachogianni, 2008: Airborne Particulate Matter and Human Health: Toxicological Assessment and Importance of Size and Composition of Particles for Oxidative Damage and Carcinogenic Mechanisms. *J. Environ. Sci. Health Part C*, **26**, 339–362, <https://doi.org/10.1080/10590500802494538>.
- 805 Wedding, J. B., and M. A. Weigand, 1993: An automatic particle sampler with beta gauging. *Air Waste*, **43**, 475–479, <https://doi.org/10.1080/1073161X.1993.10467146>.
- West Texas Mesonet, 2025: West Texas Mesonet. Accessed 15 August 2025, <https://www.mesonet.ttu.edu/>.
- Yang, S., D. Fang, and B. Chen, 2019: Human health impact and economic effect for PM2.5 exposure in typical cities. *Appl. Energy*, **249**, 316–325, <https://doi.org/10.1016/j.apenergy.2019.04.173>.
- 810 Zaidan, M. A., and Coauthors, 2020a: Intelligent Calibration and Virtual Sensing for Integrated Low-Cost Air Quality Sensors. *IEEE Sens. J.*, **20**, 13638–13652, <https://doi.org/10.1109/JSEN.2020.3010316>.
- Zhang, M., Y. Song, X. Cai, and J. Zhou, 2008: Economic assessment of the health effects related to particulate matter pollution in 111 Chinese cities by using economic burden of disease analysis. *J. Environ. Manage.*, **88**, 947–954, <https://doi.org/10.1016/j.jenvman.2007.04.019>.
- 815 Zhang, X., D. Li, and T. Bo, 2018: The variation of the vertical electric field (Ez) with height during dust storms and the effects of environmental variables on Ez. *Granul. Matter*, **20**, 33, <https://doi.org/10.1007/s10035-018-0801-6>.
- Zico da Costa, A. Z., J. P. S. Aniceto, and M. Lopes, 2024: Low-Cost Sensor Network for Air Quality Assessment in Cabo Verde Islands. *Sensors*, **24**, 7656, <https://doi.org/10.3390/s24237656>.

820